NASA TECHNICAL MEMORANDUM

NASA TM X-73401

NASA TM X-73401

D-1A EQUIPMENT MODULE STRUCTURE TEST

by T. F. Niezgoda
Lewis Research Center
Cleveland, Ohio 44135
April 1976

1. Report No NASA TM X-73401	2. Government Accession No	3 Recipient's Catalog No
4 Title and Subtitle D-1A EQUIPMENT MODULE STRUCTURE TEST		5 Report Date 6 Performing Organization Code
7. Author(s) Thomas F. Niezgoda		8 Performing Organization Report No E-8724
9. Performing Organization Name and Address Lewis Research Center National Aeronautics and Space Administration Cleveland, Ohio 44135		10 Work Unit No 11 Contract or Grant No.
12 Sponsoring Agency Name and Address National Aeronautics and Space Administration Washington, D.C. 20546		13. Type of Report and Period Covered Technical Memorandum 14. Sponsoring Agency Code
15 Supplementary Notes		

16. Abstract

The Centaur Equipment Module (E/M) structural test program was performed in two parts due to an unscheduled hardware failure in the first test series. The objectives of the initial test program were to define the flexibility characteristics of the E/M, verify the design load capability, and determine its ultimate strength capability by loading to structural failure. However, during the first failure test attempt, the Intelsat IV MPA failed instead of the E/M. Therefore a new adapter was fabricated to simulate the HEAO mission adapter and the second series of tests were then performed. They concluded with the failure of the E/M forward interface ring resulting in about 3.5 degrees of permanent set on the high compression side. Nevertheless, the linear or useable strength capability of the E/M is greater or equal to that which is required for the HEAO missions. The E/M is deemed structurally qualified for the HEAO missions.

17. Key Words (Suggested by Author(s)) Centaur Equipment module	18. Distribution Statement Unclassified - unlimited

19 Security Classif. (of this report) Unclassified	20 Security Classif. (of this page) Unclassified	21. No. of Pages	22 Price*

* For sale by the National Technical Information Service, Springfield, Virginia 22161

TABLE OF CONTENTS

ABBREVIATIONS

CSS	Centaur Standard Shroud
D-1A	Atlas/Centaur Configuration
D-1T	Titan/Centaur Configuration
EID	General Dynamics Convair Division End Item Description (Accompanied by Part Number)
E/M	Equipment Module
GDC	General Dynamics Convair Division
HEAO	High Energy Astronomical Observatory
in-lb	Inch-Pounds, Bending Moment
LeRC	Lewis Research Center, Cleveland, Ohio
LH_2	Liquid Hydrogen
MPA	Mission Peculiar Adapter
OAO	Orbiting Astronomical Observatory
P_{eq}	Equivalent Axial Load
psi	Pounds per Square Inch, Stress
SPC	Space Power Chamber at Lewis Research Center

SUMMARY

The Centaur Equipment Module (E/M) structural test program began on November 4, 1974, and was completed on April 2, 1975. However, due to an unscheduled hardware failure, the testing was performed in two programs; the first with an Intelsat IV flight-type payload adapter (mission peculiar adapter--MPA), and the second with a simulated HEAO-type payload adapter fabricated at LeRC. The objectives of the initial test program were to define the flexibility characteristics of the E/M, verify the design load capability, and determine its ultimate strength capability by loading to structural failure. During the first test program, the flexibility characteristics and the design load capability of the E/M were determined. However, as the external loads were increased during the failure load test, the forward ring mating flange of the MPA failed instead of the E/M. Therefore, the last test objective was not fulfilled.

A second test program was initiated as a result of the unscheduled MPA failure. The primary objectives of this test were to verify the flexibility characteristics derived from the first test, qualify the E/M for the HEAO mission design loads, and determine the ultimate strength capability of the E/M by loading to structural failure. This test was performed and concluded with the failure of the forward interface ring of the E/M resulting in about 3.5 degrees of permanent set on the high compression side. However, it is possible that the ultimate E/M strength capability was compromised by the simulated HEAO adapter's material (6061 aluminum) being in the annealed condition due to welding at the interface ring. Nevertheless, the linear or usable strength capability of the E/M is greater or equal to that which is required for the HEAO missions. Therefore, the E/M is deemed structurally qualified for the HEAO missions.

INTRODUCTION

The Centaur E/M is a 10-foot base diameter conical aluminum skin-stringer structure 30 inches high that is mounted on the forward end of the Centaur stub adapter (see Figure 1). Its functions are to:

1. Provide structural support for a payload adapter carrying payloads of various sizes, shapes, and weights

2. Provide mounting for various electrical/electronic components

3. Provide mounting for the electrical harnesses servicing the mounted components

4. Provide mounting for the forward umbilical panel

5. Provide mounting for electrical connectors to the nose fairing

6. Provide mounting for LH_2 balanced thrust venting system ducting and nozzles

Since the E/M is a relatively complex structure, the analytical design factors that dictated the published structural capability of the E/M needed to be confirmed. Therefore, a structural test program utilizing a Centaur E/M was initiated at LeRC.

Significant contributions and consulting services in preparing this report were provided by William M. Prati and Robert P. Miller of LeRC. James Jenness, from the contractor GDC, assisted in monitoring each test and in data reduction.

TEST OBJECTIVES

I. First Test Program

A. Determine the flexibility characteristics of the E/M

B. Verify the D-1A and D-1T design load capability

C. Determine the ultimate strength capability of the E/M by loading to structural failure

II. Second Test Program (due to unscheduled failure of test hardware during first test program)

A. Verify the previously defined flexibility matrix which was determined in the first test program

B. Qualify the E/M for all HEAO mission design loads

C. Determine the ultimate strength capability of the E/M by loading to structural failure

APPARATUS

The stackup of hardware shown in Figure 1 was used for supporting the E/M as well as for distributing the simulated flight loads by an arrangement of hydraulic actuators and linkages. A description of the various pieces of hardware, load application system, instrumentation, and data acquisition follows.

The E/M (EID 55-0592) used in these tests was the same D-1T E/M used in the LeRC Plum Brook CSS structural and jettison tests which were performed 3 years ago. However, it was modified in the LeRC fabrication shop to match the current D-1A flight configuration (GDC drawing no. 55-74800-43) as closely as possible. Some holes were drilled through the skin and equipment mounting rails for purposes of load application. The E/M is constructed in the shape of a truncated cone 30 inches high with a cone half-angle of 45 degrees. It is 120.36 inches in diameter at the base and tapers to 60.36 inches diameter at the forward end.

It consists of 2024 aluminum skin riveted to a machined ring at either end, longitudinal stiffeners riveted to the forward (outer) side of the skin, and two circular frames riveted to the aft (inner) side of the skin. Two circumferential fiberglass hat section equipment mounting rails are attached to the stiffeners. The thermal diaphragm which is normally mounted at the forward end of the E/M was not used in these tests. This opening was needed for the axial load application cable to pass through.

The E/M was bolted to the forward ring of the stub adapter. This stub adapter was also used in the LeRC Plum Brook CSS test program. It was the D-1T configuration consisting of a ring stiffened titanium skin and stringer structure 120 inches in diameter and 25 inches high.

The stub adapter was bolted to the forward end of the Agena spacer can which was used to simulate the Centaur LH_2 tank and also as an intermediate support for the test hardware. The Agena spacer can was a 120-inch diameter cylinder about 51 inches high. The bottom flange of this Agena spacer can was then bolted to the base adapter which was rigidly attached to the floor of the Space Power Chamber (SPC) wind tunnel. Internal access to the Agena spacer can was achieved through a manhole cut into the skin between two frames and longitudinal stiffeners. This access was necessary for technicians and mechanics to hook up instrumentation, axial load actuator, and package loading systems.

For the first series of tests, an Intelsat IV MPA was bolted to the forward end. This adapter was strengthened by removing the stub stringers and replacing them with full stringers which extended to the full height of the adapter, 18.75 inches. The adapter was 60.36 inches in diameter at the base and tapered to 56.26 inches diameter at the forward end. The nose fairing jettison helper spring struts were removed from the 0 degree and 180 degree azimuths and replaced at 45 degrees and 225 degrees so that the helper springs could load the adapter normal to the shear load direction.

A modified Paducah can (OAO adapter mockup) was bolted to the forward end of the Intelsat IV adapter. The strength of the Paducah can was greatly increased by adding back-to-back stringers between each of the original stringers.

For the second series of tests, i.e., after the ring failure of the Intelsat IV adapter, a new adapter was fabricated in the LeRC fabrication shop (see Figure 2). It was a 6061-T6 aluminum ring-stiffened cylinder 60.36 inches in diameter and 37.1 inches high. However, the material became annealed in the weld-affected zones near each of the flanges. The adapter aft flange was the same thickness (0.340 inches) as the current HEAO payload adapter (GDC drawing no. 55-74908) and the wall thickness was 0.187 inches instead of 0.140 inches as on the HEAO adapter. The major difference was in the material. The HEAO adapter material is 2219-T852 aluminum which is machined from a ring forging and thus has a much higher yield strength. A rolled steel angle 1/4 x 1 1/2 x 1 1/2 was bolted to the skin with the forward flange 13.00 inches above the aft flange of the adapter to simulate the forward flange of the HEAO adapter. Provision was made for attaching newly-made helper spring support longerons in line with the shear load as well as normal to the shear load.

A 3/4-inch gussett-stiffened steel plate was placed on the forward end of the Paducah can. It served the dual purpose of a load point for applying the axial loads as well as the lower shear load to the structure. It was match drilled to the forward flange of the Paducah can for through bolts to mount the OAO/Agena conical adapter on top of the stackup. This conical adapter was 45.3 inches high and tapered from 60.3 inch diameter out to 120 inches diameter at the top. The OAO/Centaur fixed fairing, a 120 inch diameter cylinder 26.8 inches high, was bolted to the top end of the Agena conical adapter with a 0.16 inch spacer between the mating flanges.

Two 8-inch I-beams welded into a cross were attached to the forward flange of the OAO/Centaur fixed fairing. It was attached by bolting through four large gussets at the four ends of the 8-inch I-beams. Brackets were welded to the I-beam for the purpose of applying the forward lateral shear force and the longitudinal counterbalance force. This loading fixture completed the stackup for supporting and applying the principal loads to the E/M. Other loads were applied with helper springs and water-lever systems.

Figures 3 and 4 illustrate the two basic stackups of structure for the first series of tests with the modified Intelsat IV MPA and the second series of tests with the simulated HEAO adapter.

The basic load application was done with hydraulic actuators in conjunction with hand-operated pumps (see Figures 3 and 4). This method allowed for a simple, reliable, and safe system. The system could and did self-relieve in the event of a structural failure. The helper spring loads were applied to the Intelsat IVA MPA with the actual flight-type helper springs. These springs were mounted to brackets which were attached to a circular work platform surrounding the hardware stackup. The second series of tests required a different setup since the new HEAO adapter was being loaded in two different perpendicular directions. A lever system was used which had a barrel on one end filled with water to apply the required forces. This force was monitored with load cell. A similar system was utilized for the counterbalance application system. A force of 3475 pounds was required to counterbalance the dead weight of the hardware above the E/M.

There were three basic types of instrumentation used for the test program, i.e., strain gages, deflectometers, and load cells. However, in order to more accurately determine the very small deflections, the use of a dial gage indicator was required in the stiffness test series.

Each deflectometer was individually calibrated over a certain range to determine its linearity and repeatibility. It was discovered that a hysteresis did exist for each pot where the direction of travel was reversed. The magnitude of this hysteresis was approximately the same for every pot (0.012 inches). Each pot was calibrated end-to-end prior to every test.

The strain gages were the typical foil-type gages wired as single active gages with temperature compensating gages mounted on separate dummy platelets. The first series of tests had strain gages mounted on the Intelsat IV MPA and stub adapter to verify good load distribution into the E/M. Figure 5 illustrates the general strain gage locations on the hardware. Figures 6 and 7 give the specific gage locations on the equipment module, the stiffeners, and skin. The

second series of tests required a new set of strain gages since the shear pull azimuth was changed from 315 degrees to 51 degrees. Figures 8, 9, and 10 give the new locations and new instrument numbers. After the gages were installed, an end-to-end check was performed up to each gage on the system with a calibrated beam.

The test data were recorded on a paper punch tape by a Vidar digital recorder. This recorder could only handle up to 48 channels of information at each data scan. Since the data were recorded in raw form, i.e., millivolts, they had to be manually reduced to engineering units. However, a computer program was prepared for the second series of tests. It could read the paper tape and convert the data to engineering units, then print the results in tabulated listings.

In addition to the Vidar digital recorder, X-Y recorders, Brush strip chart recorders, and digital volt meters were used to record and monitor the test data in real time. These real time monitoring instruments were also necessary for the test conductor to control the test loading sequence.

TEST RESULTS AND DISCUSSION

The first series of tests, begun on November 4, 1974, were done with the Intelsat IV MPA mounted on the forward ring of the E/M. There were three primary objectives to accomplish in these tests. The first set of tests in this series were performed to determine the stiffness of the forward end of the E/M with respect to shear, axial, and bending moment loads. Then a set of tests were performed to verify the structural capability of the E/M to withstand design limit and design ultimate loads. Finally, a failure load test was attempted to determine the ultimate load carrying capability of the E/M. Unfortunately it ended with a failure of the forward ring of the Intelsat IV MPA before any indication of E/M failure.

Beginning with the stiffness tests, the arrangement of shear load actuators shown in Figure 3 allowed loading the E/M with pure shear or pure bending moment. The axial load could also be applied individually. These loads were applied separately up to 80 percent of design limit while deflection measurements were taken with a dial gage at certain positions. See Tables 1, 2, and 3 and Figures 11, 12, and 13 for the tabulated values and locations of these deflection measurements. The E/M deflected linearly with load and showed good repeatability in the data. A flexibility matrix was determined from these data. A comparison of the analytical and actual flexibility matrices is shown in Figure 14, and the recommended matrix is shown at the bottom of this figure. This flexibility matrix is used to predict launch and flight loads during an Atlas/Centaur flight.

The next phase of testing consisted of loading the E/M to the D-1A design limit and design ultimate loads which are shown in Table 4. These loads were obtained by combining the axial and shear loads so that the maximum equivalent compressive axial load and maximum equivalent tensile axial load occurred in separate tests. The E/M demonstrated its design capability in each test by showing no

structural permanent set and no yielding strains. Deflections were linear with respect to load also and they were predictable to within 5 percent by using the flexibility matrix defined in the previous stiffness tests.

The first E/M failure test was attempted on December 11, 1974. Table 5 describes the loading sequence and test procedure which concluded with the ring failure at the MPA--Paducah can interface. The mode of ring failure shown in Figure 15 was attributed to the eccentric load path followed by the longitudinal line load due to bending moment and axial load. At the moment of failure, the axial load was 20,000 pounds and the shear load was 21,000 pounds which developed a bending moment of 2.411×10^6 in-lb at the forward ring of the E/M. This combined loading resulted in an equivalent axial compressive load of 180,700 pounds.

Strain gage data indicated that the E/M was responding linearly and that there was no permanent set in any of the E/M structure. Figures 16 and 17 show some stresses versus the forward shear load. Maximum normal stress of 20,874 psi occurred in the 315 degree stiffener near the forward ring of the E/M. The maximum measured shear stress of 29,684 psi occurred in the skin near the forward ring of the E/M, 90 degrees away from the shear load direction. Because of distortions in the Intelsat IV MPA, some of the deflection measurements did not provide reliable data. Table 6 summarizes all the tests performed in this series of tests with the Intelsat IV MPA.

The second series of tests with the new simulated HEAO adapter began on March 19, 1975. Figures 4 and 18 show the test setup and Table 7 lists the test procedure and loading sequence followed while performing these tests. Table 8 summarizes all the tests performed in this series of tests with the simulated HEAO adapter.

The first several tests checked out the new helper spring hydraulic loading fixture and verified the previously determined flexibility data. Strain gage data helped determine that the helper spring load was more critical to the E/M when applied in a direction perpendicular to the shear load. The first set of ultimate tests had the standard spring load of 2280 pounds, and the second set of tests had the highest spring load expected for any flight, i.e., 3500 pounds (FLTSATCOM mission). Both the standard spring loads and high spring loads were applied parallel to the shear force and perpendicular to the shear force in these tests. See Table 8 for a more descriptive summary of these tests. The E/M responded in a linear fashion throughout these tests as the deflection and stress curves from test no. 17 illustrated in Figures 19 through 22. The magnitudes of the deflections and stresses were predictable from the previous testing. Test no. 17 was chosen as a representative sample to present the data because it had the highest loading prior to the final test.

The second E/M failure strength test was performed on April 2, 1975. The 1130-pound package load was applied first, then the 3500 pound helper spring load and the 20,000 pound axial load were applied and maintained throughout the test. At this point, shear load was applied using the upper and lower actuators which resulted in an apparent moment arm of 136.6 inches above the E/M forward ring. The shear load application was continued up to a maximum force of 19,250 pounds when the deflectometer data indicated a yielding in the structure. Immediately

after recording data, the shear load was reduced and the remaining axial load, helper spring load, and package load were removed. The bending moment reached at the peak shear load point was 2.63×10^6 in-lb at the forward ring of the E/M.

Inspection of the structure after all the loads were removed revealed that the buckling of the simulated HEAO adapter on the high compression side was the point of structural failure. Figure 23 illustrates the type of buckling failure which distorted the simulated HEAO adapter ring and the forward ring of the E/M. Figure 24 is a photo of the same point showing the 11-degree ring distortion and Figure 25 is an internal view. The opposite tension side shows the 0.085 inch gap between the interface rings of the adapter and E/M shown in Figure 26. The E/M forward ring did return to 3.5 degrees when the simulated HEAO adapter was removed and the diameter returned to its original circular shape with no permanent set. Figure 27 shows the axial deflection of the forward end of the E/M on the compression and tension sides and gives an indication of symmetrical plane rotation. Figure 28 shows the E/M forward ring plane rotation and compares it to the predicted values. The test values are in good agreement with the predicted loads up to about 13,000 pounds of shear where significant nonlinear deflection began to occur. The stiffener stresses indicated a linear response to loading, in general, except for the points near the forward end of the E/M reflecting the distortion of the adapter ring and E/M forward ring. Figures 29 through 31 illustrate the strain gage data versus load for some of the more significant stiffeners at the high compression azimuth and the highest tension azimuth. The maximum shear stress measured occurred in the skin at the 324 degree azimuth near the forward E/M ring (see Figure 9), and its value was 35,750 psi.

Figure 32 compares the maximum test loads which were applied to the E/M in the two failure tests to the HEAO mission predicted maximum flight loads. As this figure indicates, the E/M supported loads well in excess of these loads and is structurally qualified for these missions.

SUMMARY OF RESULTS

The E/M structural tests established the E/M flexibility characteristics and demonstrated design strength capability as well as ultimate strength capability by continued loading to structural failure. There were two different testing configurations used; the first was the modified Intelsat IV MPA, and the second was with the LeRC-fabricated simulated HEAO adapter

RESULTS WITH INTELSAT IV MPA

1. The flexibility matrix defining the response characteristics of the E/M to shear, axial, and bending moment was determined. This was done by applying individual loads up to 80 percent of design limit while recording deflections at the required locations.

2. The E/M was loaded to ultimate design load with smooth linear response and good repeatability and no yielding or permanent set.

3. The ultimate strength failure test was performed resulting in the failure of the Intelsat IV MPA instead of the E/M. The loading at the moment of failure was:

$$\text{Bending moment} = 2.41 \times 10^6 \text{ in-lb}$$

$$\text{Compressive } P_{eq} = 180.7 \times 10^3 \text{ lb}$$

$$\text{Tensile } P_{eq} = 140.7 \times 10^3 \text{ lb}$$

RESULTS WITH SIMULATED HEAO ADAPTER

1. The previously defined flexibility matrix was verified.

2. The E/M was loaded to limit and design ultimate for the HEAO satellite missions in various combinations of standard and high helper springs either perpendicular or parallel to the applied shear load. The E/M again exhibited good linear response and no structural yielding.

3. The ultimate strength failure test was performed resulting in the E/M forward ring failure indicated by the permanent set in the ring (3.5 degrees of ring roll). The maximum loads at the E/M forward ring were:

$$\text{Bending moment} = 2.63 \times 10^6 \text{ in-lb}$$

$$\text{Compressive } P_{eq} = 195.3 \times 10^3 \text{ lb}$$

$$\text{Tensile } P_{eq} = 155.3 \times 10^3 \text{ lb}$$

CONCLUDING REMARKS

Although the E/M forward ring did indicate a structural failure by rolling and being permanently set at 3.5 degrees, it is possible that the ultimate strength of the E/M was compromised by the simulated HEAO adapter mounted on the forward ring of the E/M. The 6061 aluminum of the simulated HEAO adapter was in the annealed condition at the interface of the E/M forward ring due to welding of its aft flange. This drastically reduced the yield strength of the adapter in this region and could have precipitated the ring roll due to the high compression at the point of failure. This possibility is suggested by the fact that the HEAO adapter's ring remained at about 11 degrees after being separated from the E/M while the E/M ring sprang back to about 3.5 degrees. Also, the adapter gapped at the high tension side and remained permanently set while the E/M ring had very little indication of any yielding on the high tension side.

Previously, it was noted that the simulated HEAO adapter had provision for mounting the helper spring longerons every 90 degrees on the skin of the adapter. Part of this provision was several drilled holes through the skin at these points, and during this failure test, the helper spring fixture was mounted perpendicularly to the applied shear load. This left the high compression side unsupported and the stress concentration at these holes could have caused the skin to yield and buckle, thus precipitating the ring roll. Therefore, the E/M might have supported more load than this test indicated.

However, these two series of tests may still be considered as having qualified the Centaur E/M for the HEAO satellite missions which have the highest predicted flight loads at present. The E/M withstood these loads when carried up to ultimate values with no indicated yielding or elastic buckling. The use of high-strength helper springs with their accompanied greater loads have also been qualified for the missions where their use is required.

LEWIS RESEARCH CENTER

CENTAUR EQUIPMENT MODULE STRUCTURAL TEST (@ SFC)
STIFFNESS TEST PHASE
AXIAL LOAD TEST $P_1 = 3,480$ LB., P_2 = AXIAL LOAD, $P_3 = P_4 = P_5 = 0$
11-7-74 ; 11-8-74

AXIAL LOAD (P_2) (LBS.)	DEFLECTIONS MEASURED WITH DIAL GAGE INDICATOR (INCHES)																					
	*d3	d3	d3	d3	d3	d3	d3	d3	d4	d4	d4	d4	d4	d4	d5	d6	d7	d7	d7	d8	d8	d8
0	0	0	0	0	0	0	0	0	0	0	0	0	0	0	0	0	0	0	0	0	0	0
5000	.0008	.0005	.0013	.0005	.0005	.0005	.0005	.0006	0	0	-.0007	0	-.0002	+.0001	.0075	.0058	-.0081	-.0082	-.0085	-.0062	-.0068	-.0069
10000	.0014	.0010	.0014	.0008	.0008	.0006	.0010	.0012	-.0002	-.0004	-.0005	-.0003	-.0003	-.0001	.0175	.0112	-.0150	-.0150	-.0162	-.0132	-.0135	-.0132
15000	.0015	.0015	.0016	.0010	.0013	.0005	.0010	.0012	0	0	-.0004	-.0002	-.0002	0	.0245	.0165	-.0210	-.0210	-.0235	-.0202	-.0200	-.0210
20000	.0016	.0015	.0015	.0012	.0010	.0005	.0012	.0015	0	0	0	0	+.0002	+.0002	.0315	.0225	-.0270	-.0270	-.0305	-.0272	-.0267	-.0260
15000	.0020	.0021	.0022	.0018	.0015	.0012	.0012	.0021	-.0011	-.0011	-.0012	-.0010	-.0010	-.0010	.0245	.0164	-.0210	-.0200	-.0235	-.0222	-.0205	-.0203
10000	.0020	.0025	.0026	.0020	.0016	.0012	.0018	.0020	-.0011	-.0012	-.0015	-.0012	-.0015	-.0012	.0175	.0109	-.0135	-.0125	-.0162	-.0165	-.0143	-.0142
5000	.0019	.0021	.0023	.0018	.0015	.0010	.0020	.0012	-.0012	-.0012	-.0016	-.0015	-.0016	-.0013	.0095	.0057	-.0107	-.0070	-.0082	-.0085	-.0074	-.0072
0	0	.0010	.0012	.0005	.0005	0	.0014	0	-.0007	-.0010	-.0014	-.0012	-.0012	-.0012	0	0	0	0	0	-.0010	0	0

*SEE INSTRUMENTATION SKETCH FOR LOCATION AND DIRECTIONS FOR THESE MEASUREMENTS ~ FIGURE 11

TABLE 1

LEWIS RESEARCH CENTER

CENTAUR EQUIPMENT MODULE STRUCTURAL TEST (@ SPC)
STIFFNESS TEST PHASE
SHEAR LOAD TEST $P_1 = 3{,}480$ LB., $P_2 = 0$, $P_3 > P_4$, $P_5 = 0$
11-13-74

$(P_3 - P_4)$

SHEAR LOAD (LBS.)	DEFLECTIONS MEASURED WITH DIAL GAGE INDICATOR (INCHES)								
	*d3	d4	d5	d5	d6	d7	d7	d8	d8
0	0	0	0	0	0	0	0	0	0
2000	-.0018	-.0026	-.0010	-.0018	.0025	0	0	-.0005	-.0006
4000	-.0042	-.0058	-.0035	-.0040	.0052	.0002	.0001	-.0015	-.0012
6000	-.0068	-.0090	-.0050	-.0058	.0079	.0004	-.0002	-.0018	-.0018
4000	-.0052	-.0058	-.0030	-.0035	.0049	.0002	-.0001	-.0011	-.0012
2000	-.0028	-.0028	+.0002	-.0005	.0015	.0001	0	-.0005	-.0006
0	0	0	+.0010	+.0010	-.0008	0	0	0	0

* SEE INSTRUMENTATION SKETCH FOR LOCATION AND DIRECTIONS FOR THESE MEASUREMENTS - FIGURE 11

TABLE 2

LEWIS RESEARCH CENTER

CENTAUR EQUIPMENT MODULE STRUCTURAL TEST (@ SPC)
STIFFNESS TEST PHASE
BENDING MOMENT TEST $P_1 = 3{,}480$ LB., $P_2 = 0$, $P_3 = P_4$, $P_5 = 0$
11-13-74

BENDING MOMENT** (IN-LB)	DEFLECTIONS MEASURED WITH DIAL GAGE INDICATOR (INCHES)												
	*d3	d3	d3	d4	d4	d5	d5	d6	d6	d7	d7	d8	d8
0	0	0	0	0	0	0	0	0	0	0	0	0	0
155.5×10^3	-.0005	-.0002	-.0002	-.0021	-.0022	-.0275	-.0280	.0275	.0275	-.0008	-.0010	-.0003	-.0002
311.0×10^3	-.0012	-.0010	-.0007	-.0051	-.0051	-.0577	-.0580	.0572	.0575	-.0006	-.0008	+.0018	+.0018
466.0×10^3	-.0030	-.0020	-.0019	-.0090	-.0090	-.0890	-.0833	.0850	.0850	+.0005	+.0005	.0051	.0057
311.0×10^3	-.0022		-.0010	-.0061	-.0059	-.0617	-.0580	.0570		.0005	.0005	.0031	.0030
155.5×10^3	-.0015		-.0004	-.0029	-.0028	-.0320	-.0300	.0275		.0002	.0002	.0012	.0006
0	-.0011		0	0	0	+.0002	+.0002	0		.0001	0	.0007	.0002

* SEE INSTRUMENTATION SKETCH FOR LOCATION AND DIRECTIONS FOR THESE MEASUREMENTS ~ FIGURE 11

** BENDING MOMENT IS CONSTANT OVER LENGTH OF EQUIPMENT MODULE

TABLE 3

DESIGN LOADS FOR D-1A

S/C WT. LB.	C.G. LOCATION IN.	LOAD FACTORS G's		LIMIT LOADS ON FWD. END OF E/M				
		LAT'L.	AXIAL	SHEAR LB.	MOMENT IN-LB.	AXIAL LB.	P_{EQ} COMP.	P_{EQ} TEN.
4000	85.0 FWD. TOP OF E/M	+2.0	+2.5	8000	680,000	10,000	54,000LB.	34,000LB.
		-2.0	0	8000	680,000	0	44,000LB.	44,000LB.

DESIGN LOADS FOR D-1T

S/C WT. LB.	C.G. LOCATION IN.	LOAD FACTORS G's		LIMIT LOADS ON FWD. END OF E/M				
		LAT'L.	AXIAL	SHEAR LB.	MOMENT IN-LB.	AXIAL LB.	P_{EQ} COMP.	P_{EQ} TEN.
4000	85.0 FWD. TOP OF E/M	+1.3	+6.0	5,200	441,000	24,000	54,500LB.	4,500LB.
		-1.3	-2.5	5,200	441,000	-10,000	18,500LB.	-38,500LB.

TABLE 4 EQUIPMENT MODULE DESIGN LOADS

TABLE 5

E/M D-1A CONFIGURATION STRUCTURAL FAILURE TEST WITH INTELSAT IV ADAPTER
TEST PROCEDURE AND LOADING SEQUENCE

J.O. _____
DATE _____
ENG. _____

DATA POINT	P_1 COUNTER-BALANCE LB.	P_2 AXIAL LOAD LB.	P_3 LOWER SHEAR LB.	P_4 FORWARD SHEAR LB.	P_5 PACKAGE LOAD LB.	HELPER SPRING LB.	MOMENT IN-LB. $\times 10^{-6}$	P_{EQ} TENSION LB. $\times 10^{-3}$	P_{EQ} COMPR. LB. $\times 10^{-3}$
1	3500	0	0	0	0	0	0	0	0
2		0		0	0	1620	0	0	0
3		0		0	1130		0	0	0
4		20,000		0			0	0	20.0
5				1000			0.115	0	27.67
6				2000			0.230	0	35.33
7				3000			0.344	2.93	42.93
8				4000			0.459	10.60	50.60
9				5000			0.574	18.27	58.27
10				6000			0.689	25.93	65.93
11				7000			0.804	33.60	73.60
12				8000			0.918	41.20	81.20
13				9000			1.033	48.87	88.87
14				10,000			1.148	56.53	96.53
15				11,000			1.263	64.20	104.2
16				12,000			1.378	71.87	111.9
17				13,000			1.492	79.47	119.5
18				14,000			1.607	87.13	127.1
19				15,000			1.722	94.80	134.8
20				16,000			1.837	102.5	142.5
21				17,000			1.952	110.1	150.1
22				18,000			2.066	117.7	157.7
23				19,000			2.181	125.4	165.4
24				20,000			2.296	133.1	173.1
25				21,000			2.411	140.7	180.7
INTELSAT IV ADAPTER FAILED @ V = 21,000 LB.									
26				16,000			1.837	102.5	142.5
27				12,000			1.378	71.87	111.9
28				5,000			0.574	18.27	58.27
29		20,000		0			0	0	20.0
30		0		0	1130		0	0	0
31		0		0	0	1620	0	0	0
32	3500	0	0	0	0	0	0	0	0

TABLE 6

SUMMARY OF TESTS PERFORMED WITH

INTELSAT IV MPA

SHEAR-PULL AZIMUTH AT 315 DEGREES

Test No.	Description	P_{eq} ($Lb. \times 10^{-3}$)
1 through 16 (stiffness test phase)	Axial Load Test	20.0
	Shear Load Test	6.0 (shear)
	Bending Moment Test	30.8
17	Compression Case (D-1A Loads)	67.3
18	Tension Case (D-1A Loads)	54.7
19	Compression Case (D-1T Loads)	65.6
20	Unit Loads (Strain Calibration)	
21	D-1A Capability	111.6
22	Failure Test	180.3

TABLE 7

E/M D-1A CONFIGURATION STRUCTURAL FAILURE TEST WITH SIMULATED HEAD ADAPTER

J.O. _____

DATE _____

TEST PROCEDURE AND LOADING SEQUENCE

ENG. _____

DATA POINT	P_0 FORWARD SHEAR LB.	P_1 AXIAL LOAD LB.	P_2 LOWER SHEAR LB.	P_3 PACKAGE LOAD LB.	$1.229P_{48}$ HELPER SPRING LB.	NET SHEAR LB.	MOMENT IN-LB. $\times 10^{-6}$	P_{EQ} TENSION LB. $\times 10^{-3}$	P_{EQ} COMPR. LB. $\times 10^{-3}$
0	0	0	0	0	0	0	0	0	0
1	0	0	0	1130	0	0	0	0	0
2	0	0	0	↑	1135	0	0	0	0
3	0	0	0		2270	0	0	0	0
4	0	0	0		2837	0	0	0	0
5	0	10,000	0		↑	0	0	0	10.0
6	0	20,000	0			0	0	0	20.0
7	4810	↑	1054			3756	0.513	14.2	54.2
8	9619		2107			7512	1.026	48.4	88.4
9	12,024		2634			9390	1.283	65.5	105.5
10	13,226		2897			10,329	1.411	74.1	114.1
11	14,429		3161			11,268	1.539	82.6	122.6
12	15,631		3424			12,207	1.668	91.2	131.2
13	16,834		3688			13,146	1.796	99.7	139.7
14	18,517		4056			14,461	1.975	111.7	151.7
15	20,638		4462			16,176	2.210	127.3	167.3
16	22,405		4908			17,497	2.390	139.3	179.3
17	24,646		5399			19,247	2.629	155.3	195.3
SIMULATED HEAD ADAPTER FAILED AT THIS POINT									
18	22,400	↓	5768			16,632	2.272	131.5	171.5
19	14,340		3184			11,156	1.524	81.6	121.6
20	0	20,000	0		↓	0	0	0	20.0
21	0	0	0	↓	2837	0	0	0	0
22	0	0	0	1130	0	0	0	0	0
23	0	0	0	0	0	0	0	0	0

NASA-C-801B (10-24-51)

NOTE: P_4, THE COUNTERBALANCE FORCE, WAS SET @3475 LB. THROUGHOUT TEST

TABLE 8

SUMMARY OF TESTS PERFORMED WITH SIMULATED HEAO ADAPTER

TEST NO.	DESCRIPTION	P_{eq} (LB. x 10^{-3})	HELPER SPRING CONFIGURATION
7	Limit Compression	100.4	Standard Springs Perpendicular to Shear (2280 lbs.)
8	Ultimate Compression	138.3	
9	Ultimate Tension	119.9	
10	Limit Compression	100.4	Standard Springs Parallel to Shear (2280 lbs.)
11	Ultimate Compression	138.3	
12	Ultimate Tension	119.9	
13	Limit Compression	100.4	High Springs Parallel to Shear (3500 lbs.)
14	Ultimate Compression	138.3	
15	Ultimate Tension	119.9	
16	Limit Compression	100.4	High Springs Perpendicular to Shear (3500 lbs.)
17	Ultimate Compression	138.3	
18	Ultimate Tension	119.9	
19	Failure Test	195.3	

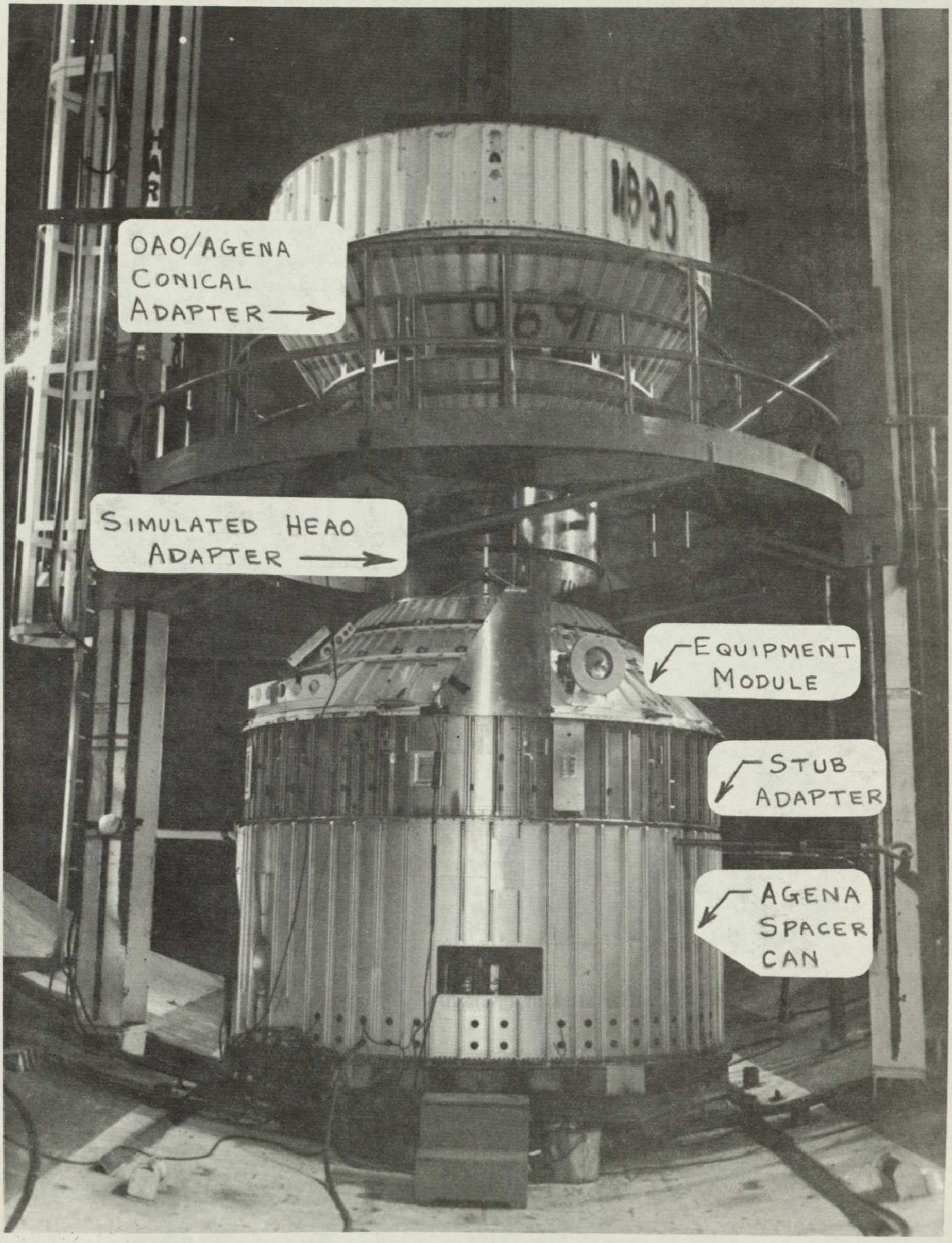

FIGURE 1 - E/M STRUCTURE TEST CONFIGURATION IN SPC

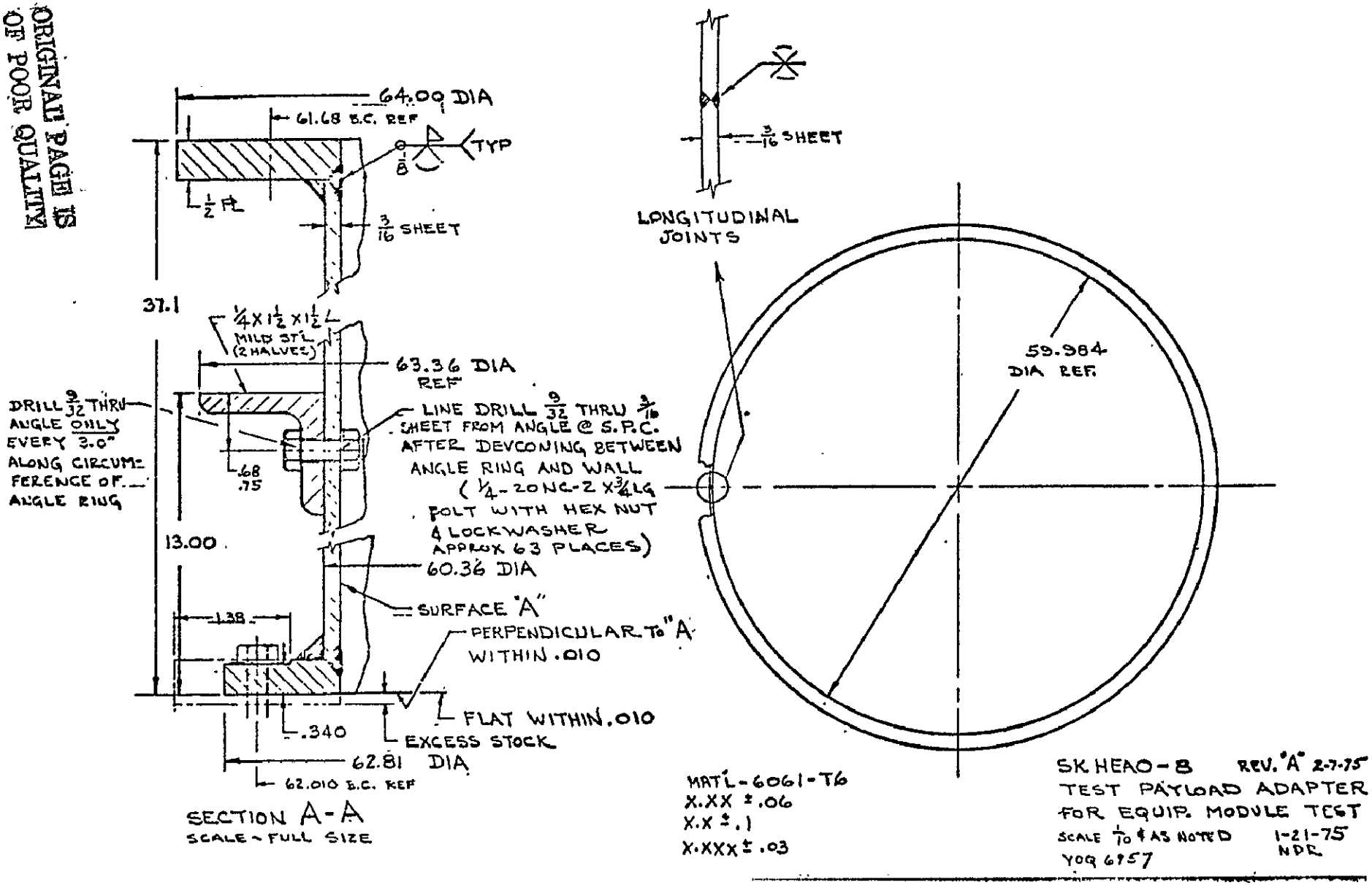

FIGURE 2 LERC FABRICATED SIMULATED HEAO ADAPTER

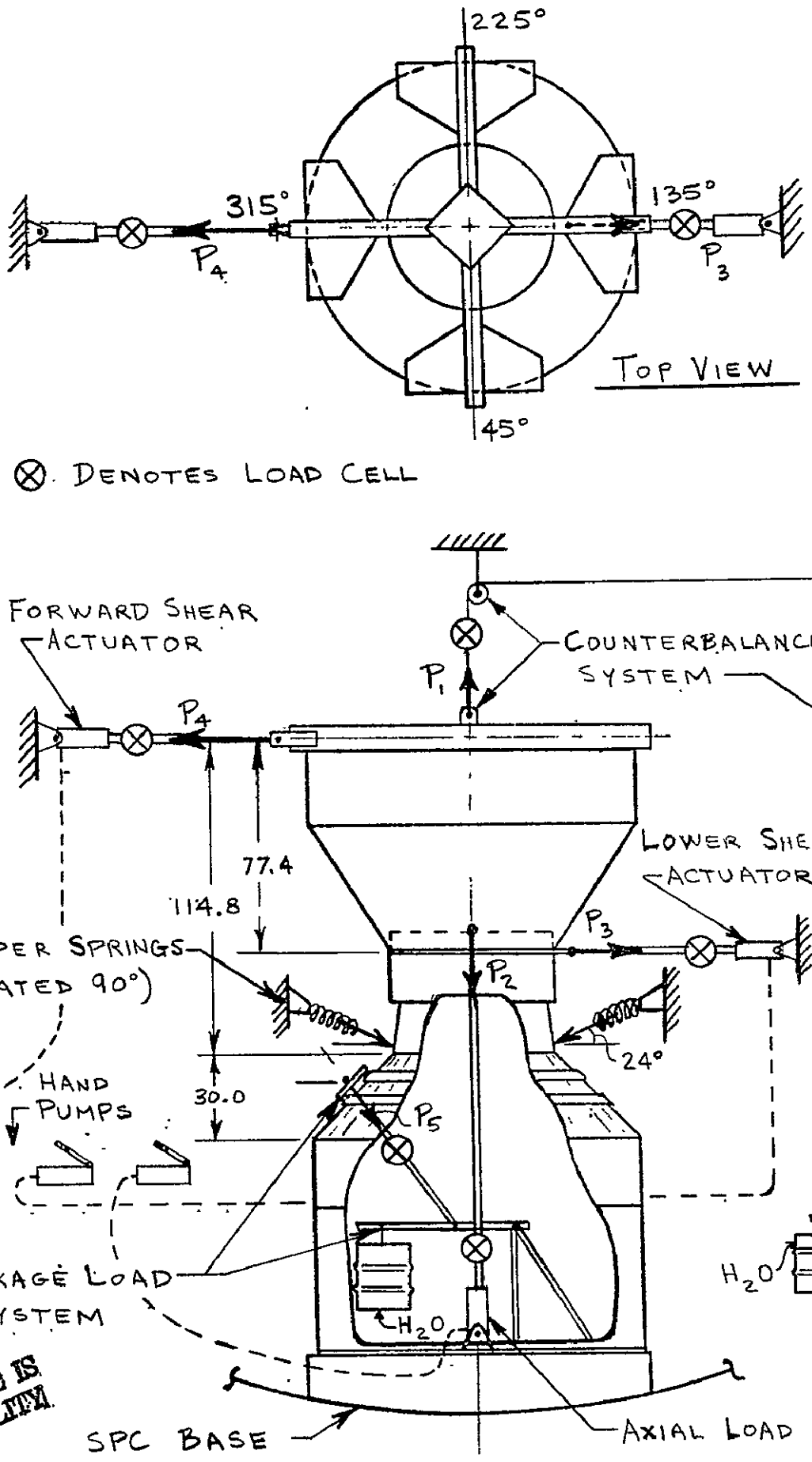

FIGURE 3 EQUIPMENT MODULE TEST LOADING SYSTEM USING INTELSAT IV ADAPTER

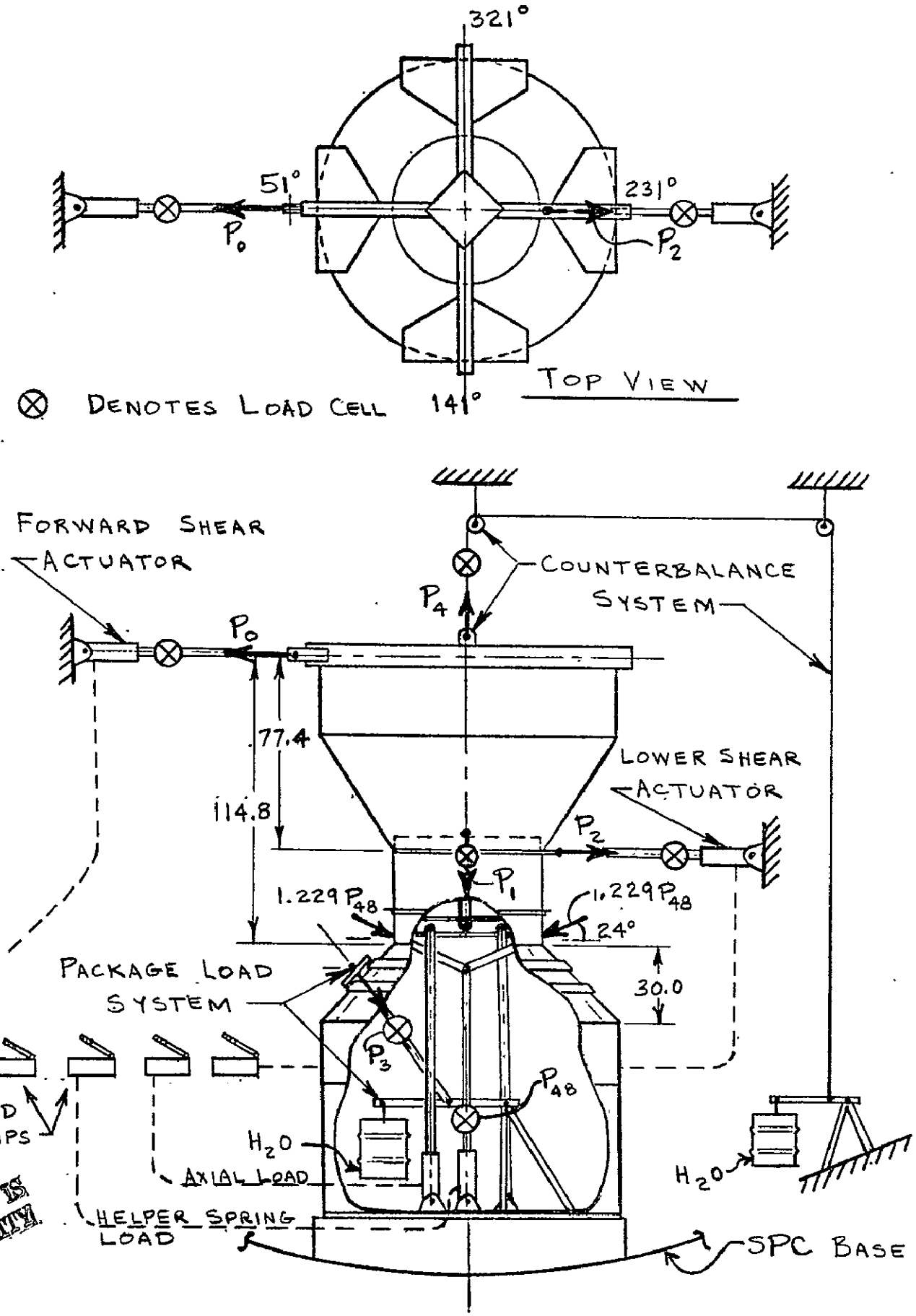

FIGURE 4 EQUIPMENT MODULE TEST LOADING SYSTEM USING SIMULATED HEAO MISSION ADAPTER

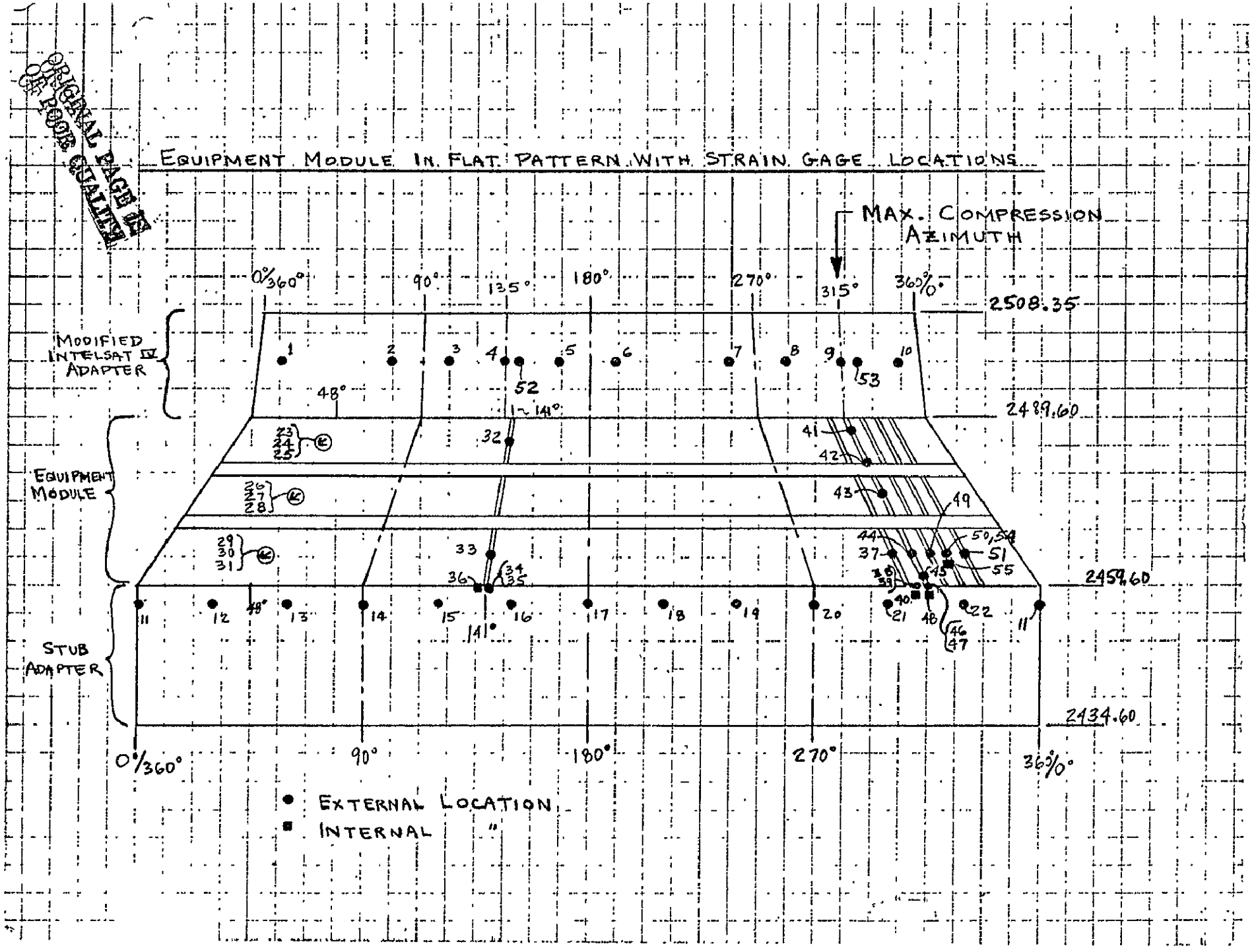

FIGURE 5 GENERAL STRAIN GAGE LOCATIONS FOR TEST WITH INTELSAT IV MPA

EQUIPMENT MODULE ROSETTE STRAIN GAGES

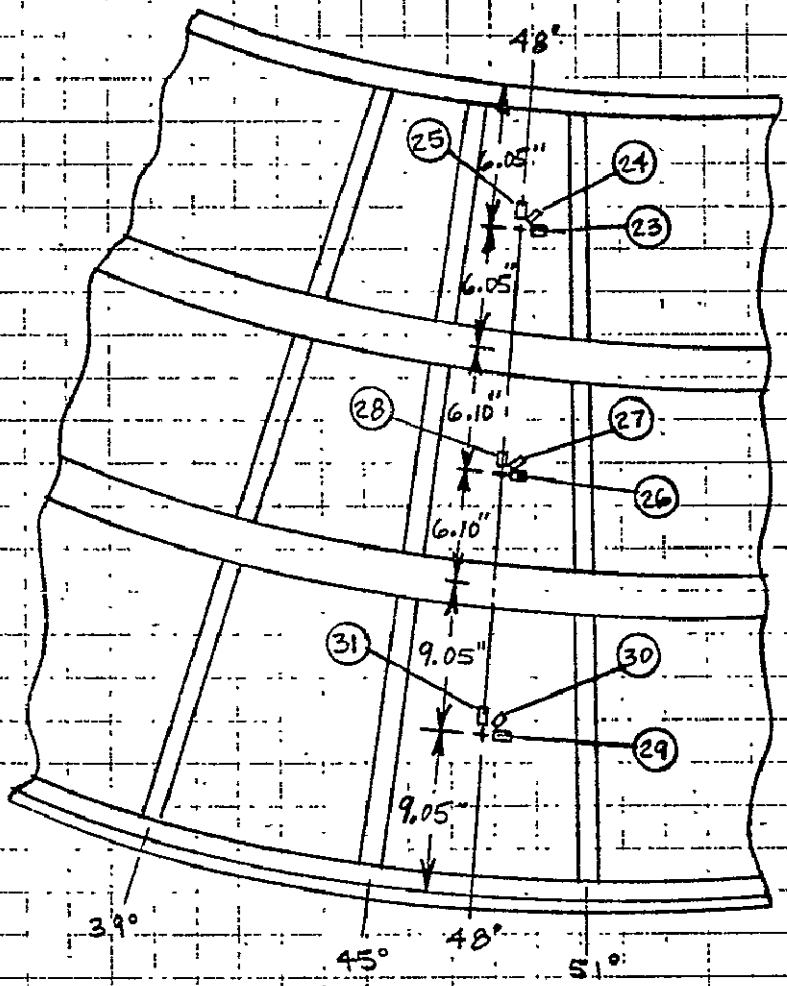

FIGURE 6 ROSETTE STRAIN GAGE LOCATIONS ON E/M FOR TEST WITH INTELSAT IV MPA

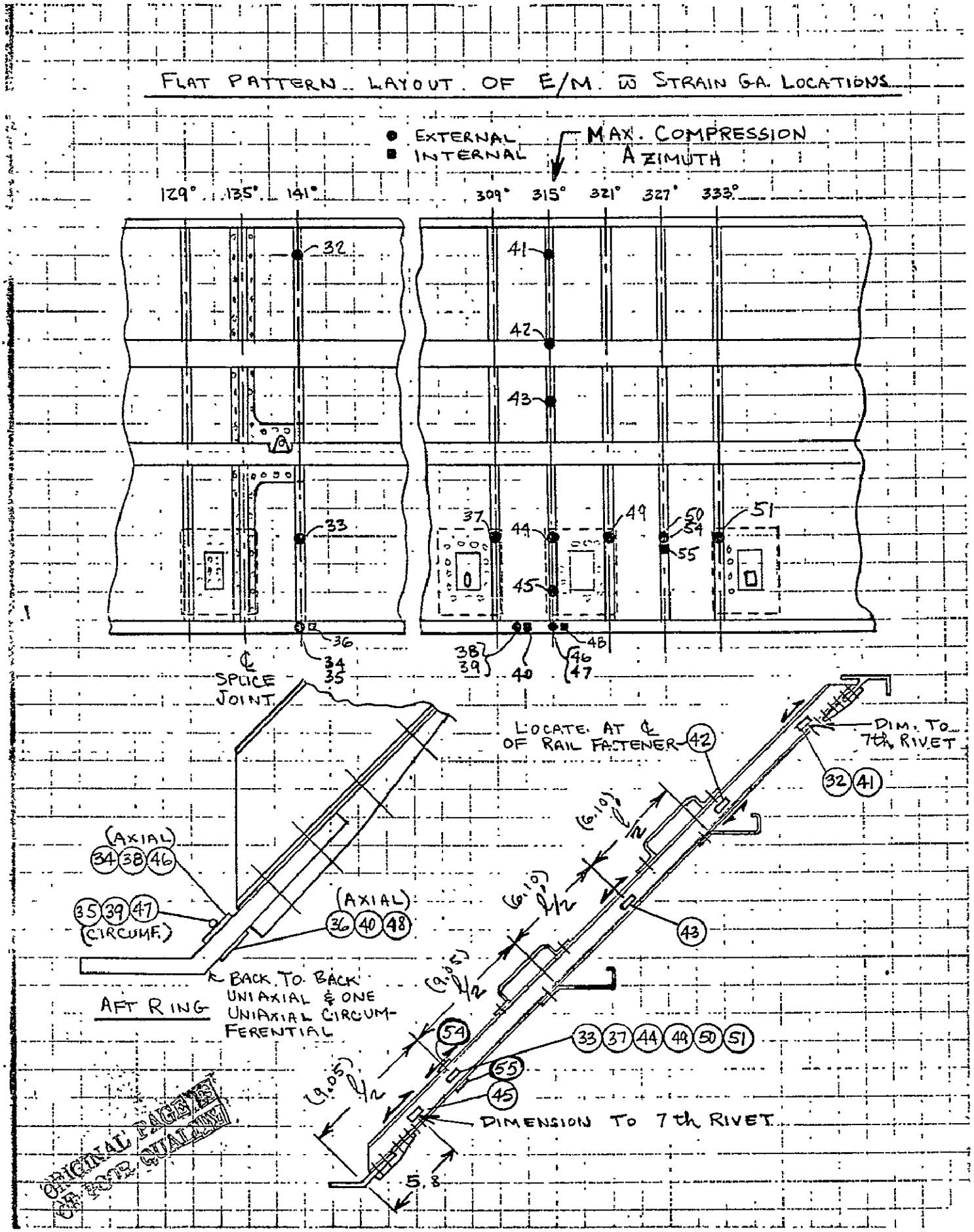

FIGURE 7 STRAIN GAGE LOCATIONS ON E/M FOR TEST WITH INTELSAT IV MPA

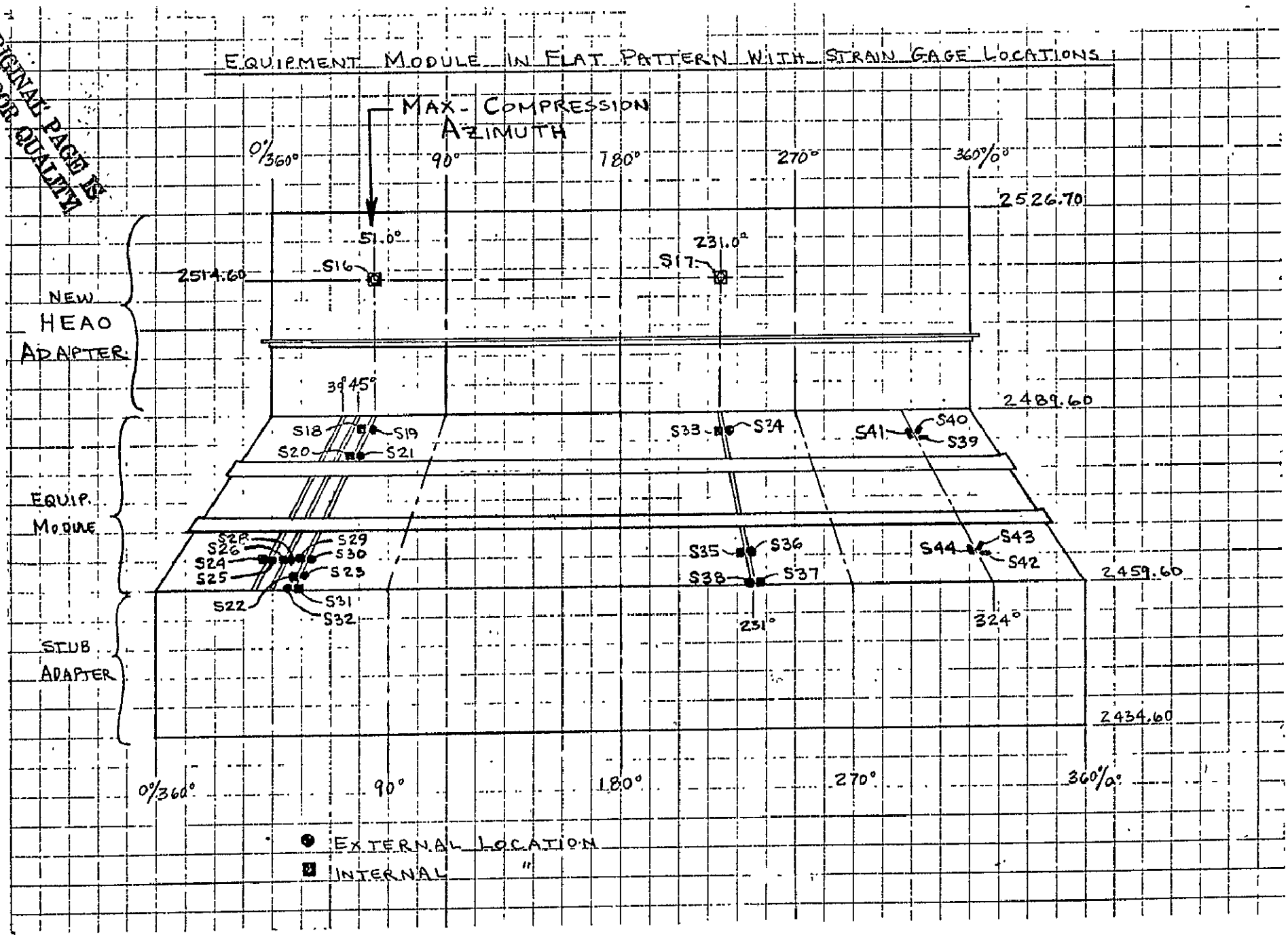

FIGURE 8 GENERAL STRAIN GAGE LOCATIONS FOR TEST WITH HEAO ADAPTER

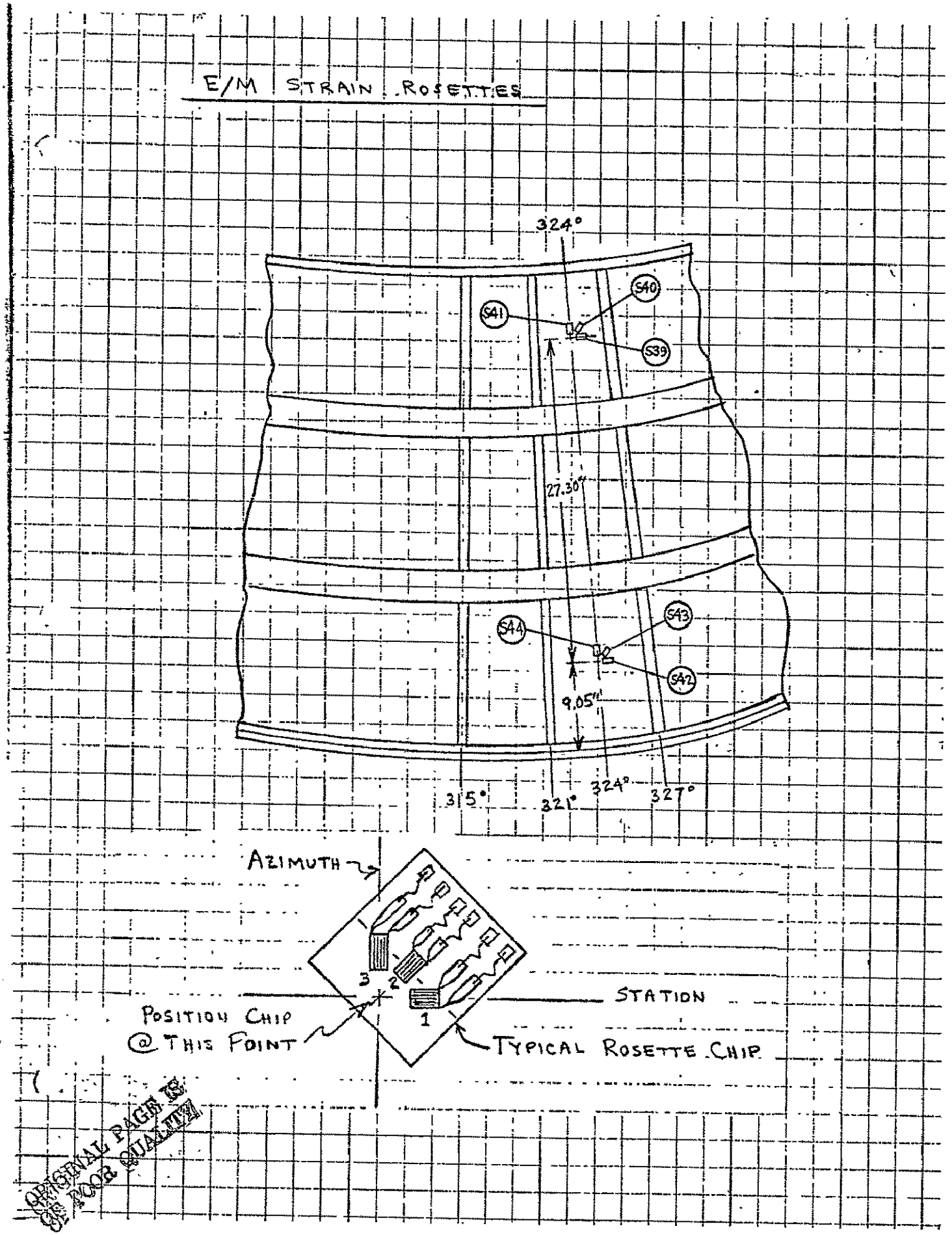

FIGURE 9 ROSETTE STRAIN GAGE LOCATIONS ON E/M FOR TEST WITH HEAO ADAPTER

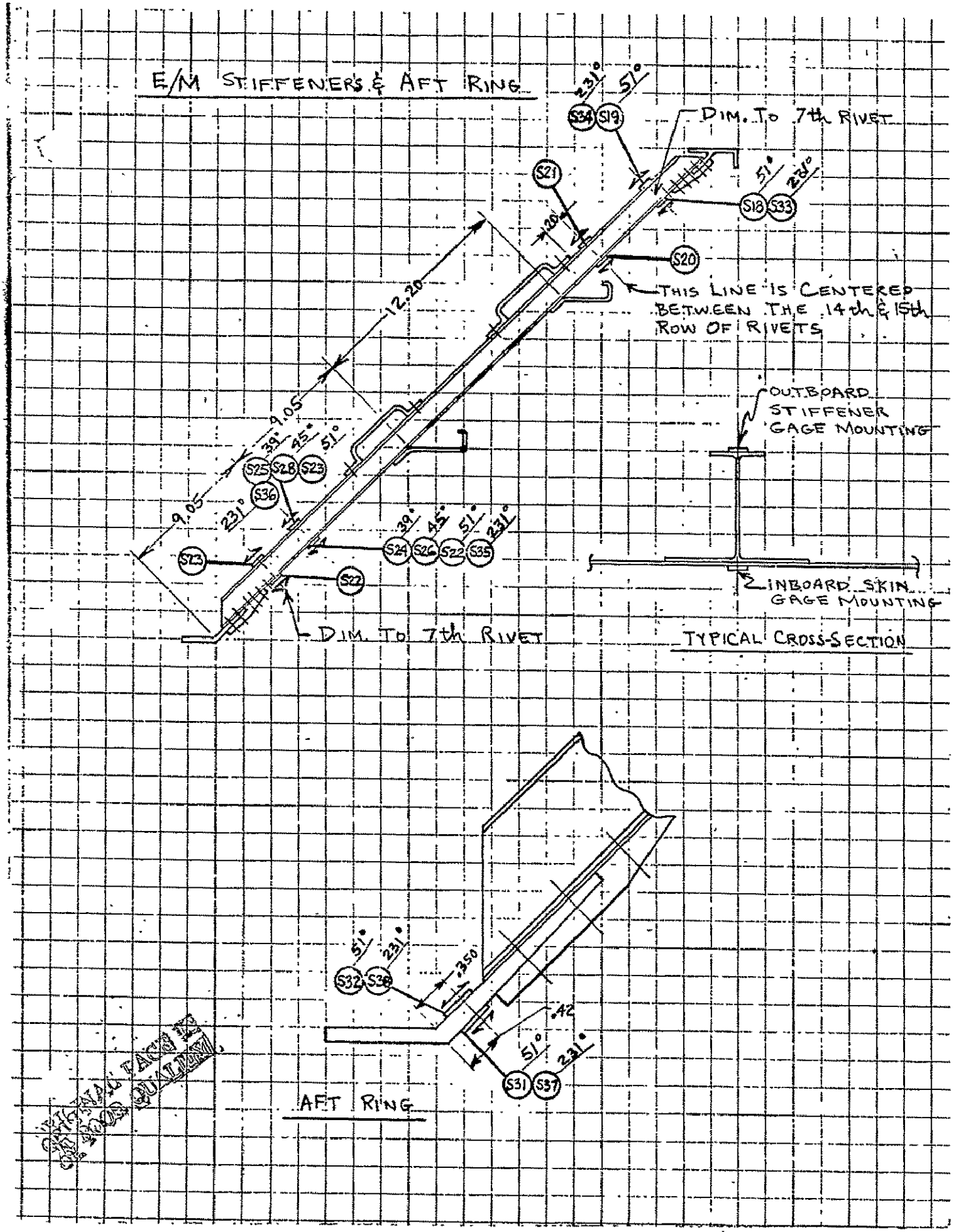

FIGURE 10 STRAIN GAGE LOCATIONS ON E/M FOR TEST WITH HEAD ADAPTER

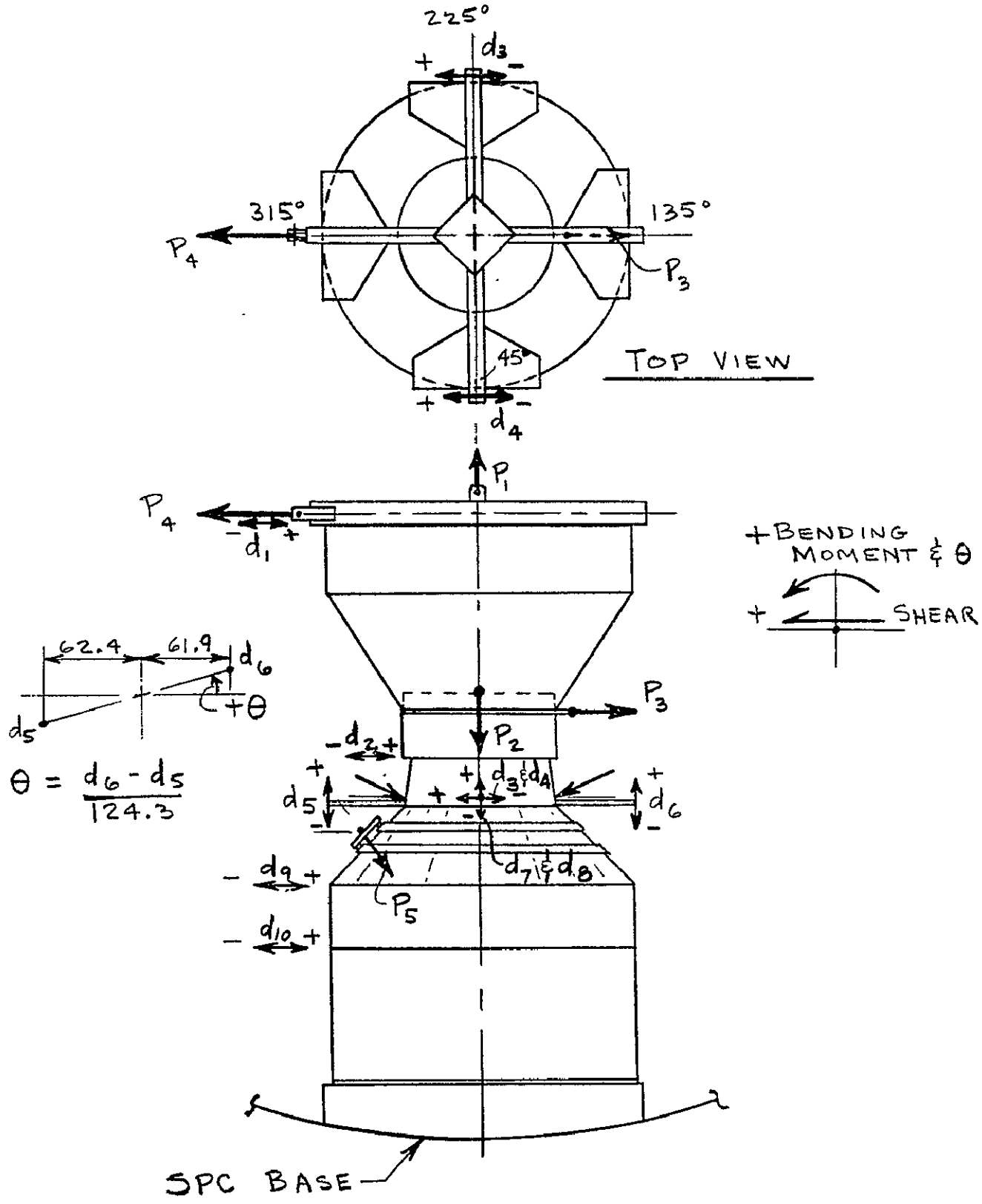

FIGURE 11 EQUIPMENT MODULE TEST WITH INTELSAT IV ADAPTER SHOWING DEFLECTOMETER LOCATIONS

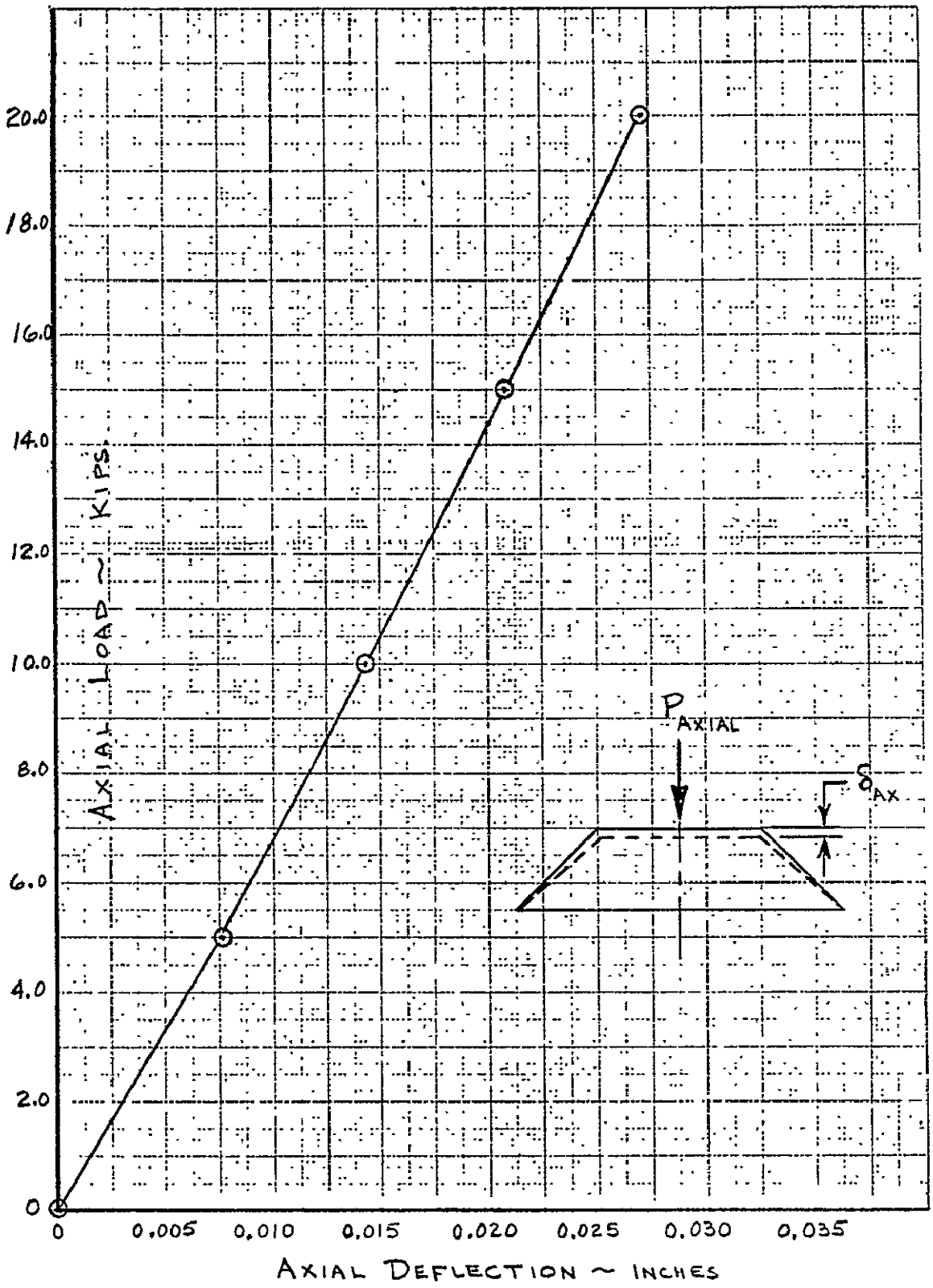

FIGURE 12 AXIAL DEFLECTION VS. AXIAL LOAD WITH INTELSAT IV ADAPTER

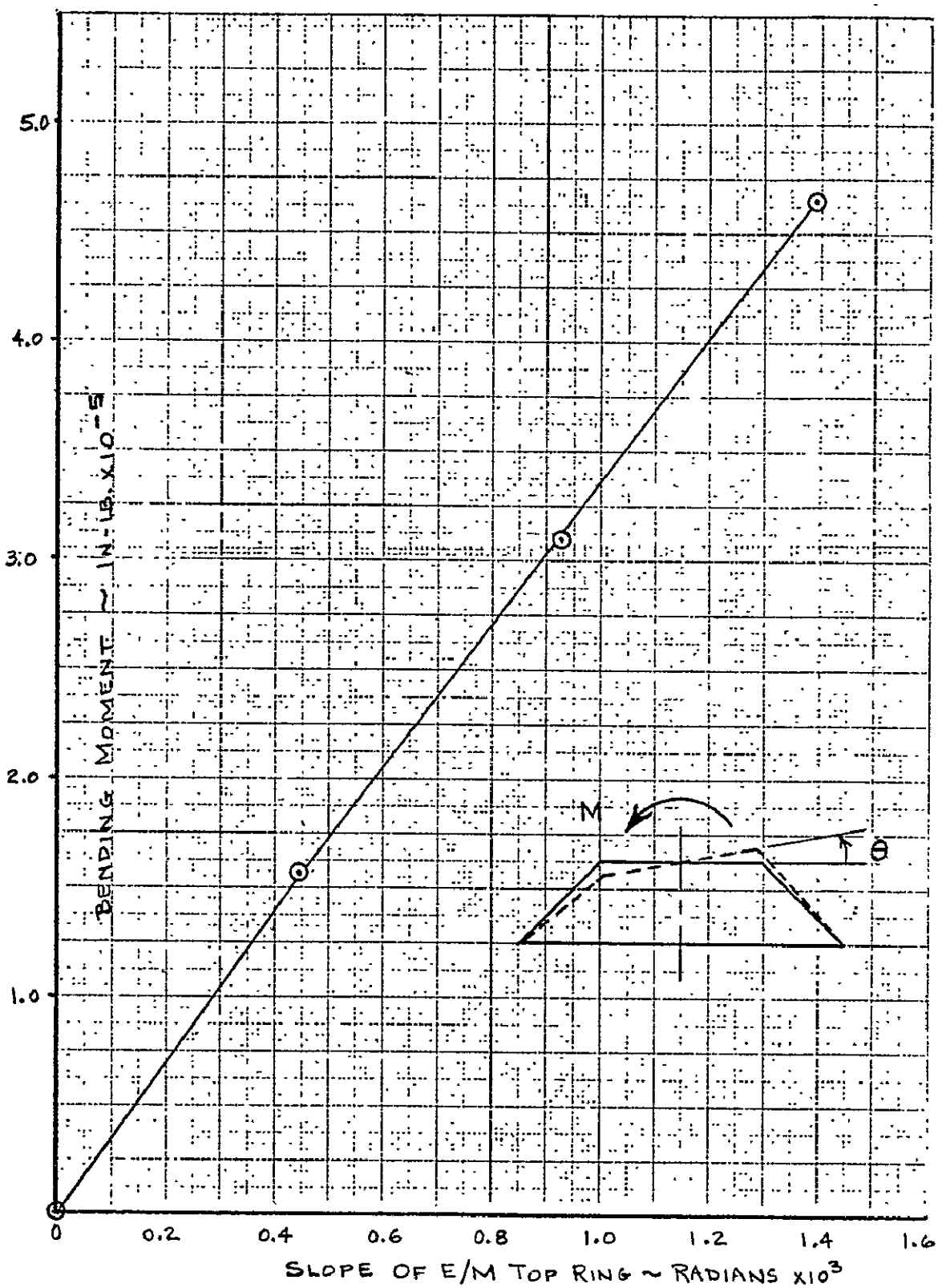

FIGURE 13 ROTATION OF E/M FORWARD RING VS. BENDING MOMENT WITH INTELSAT IV ADAPTER

ANALYTICAL FLEXIBILITY:

$$\begin{Bmatrix} \delta_V \\ \delta_P \\ \theta_M \end{Bmatrix} = 10^{-8} \begin{bmatrix} 176 & 0 & -2.0 \\ 0 & 248 & 0 \\ -2.0 & 0 & 0.35 \end{bmatrix} \begin{Bmatrix} V \\ P \\ M \end{Bmatrix}$$

MEASURED FLEXIBILITY:

$$\begin{Bmatrix} \delta_V \\ \delta_P \\ \theta_M \end{Bmatrix} = 10^{-8} \begin{bmatrix} 127 & 0 & -1.54 \\ 13.4 & 130 & -0.05 \\ -1.75 & 0.16 & 0.328 \end{bmatrix} \begin{Bmatrix} V \\ P \\ M \end{Bmatrix}$$

SUGGESTED PRACTICAL FLEXIBILITY MATRIX:

$$\begin{Bmatrix} \delta_V \\ \delta_P \\ \theta_M \end{Bmatrix} = 10^{-8} \begin{bmatrix} 127 & 0 & -1.65 \\ 0 & 130 & 0 \\ -1.65 & 0 & 0.33 \end{bmatrix} \begin{Bmatrix} V \\ P \\ M \end{Bmatrix}$$

SIGN CONVENTION:

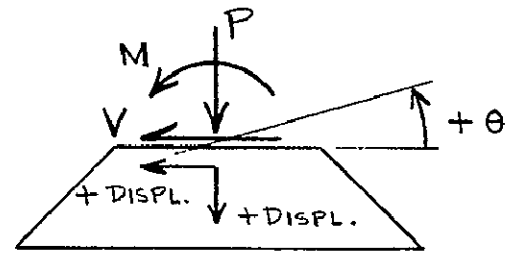

FIGURE 14 ANALYTICAL AND MEASURED FLEXIBILITY

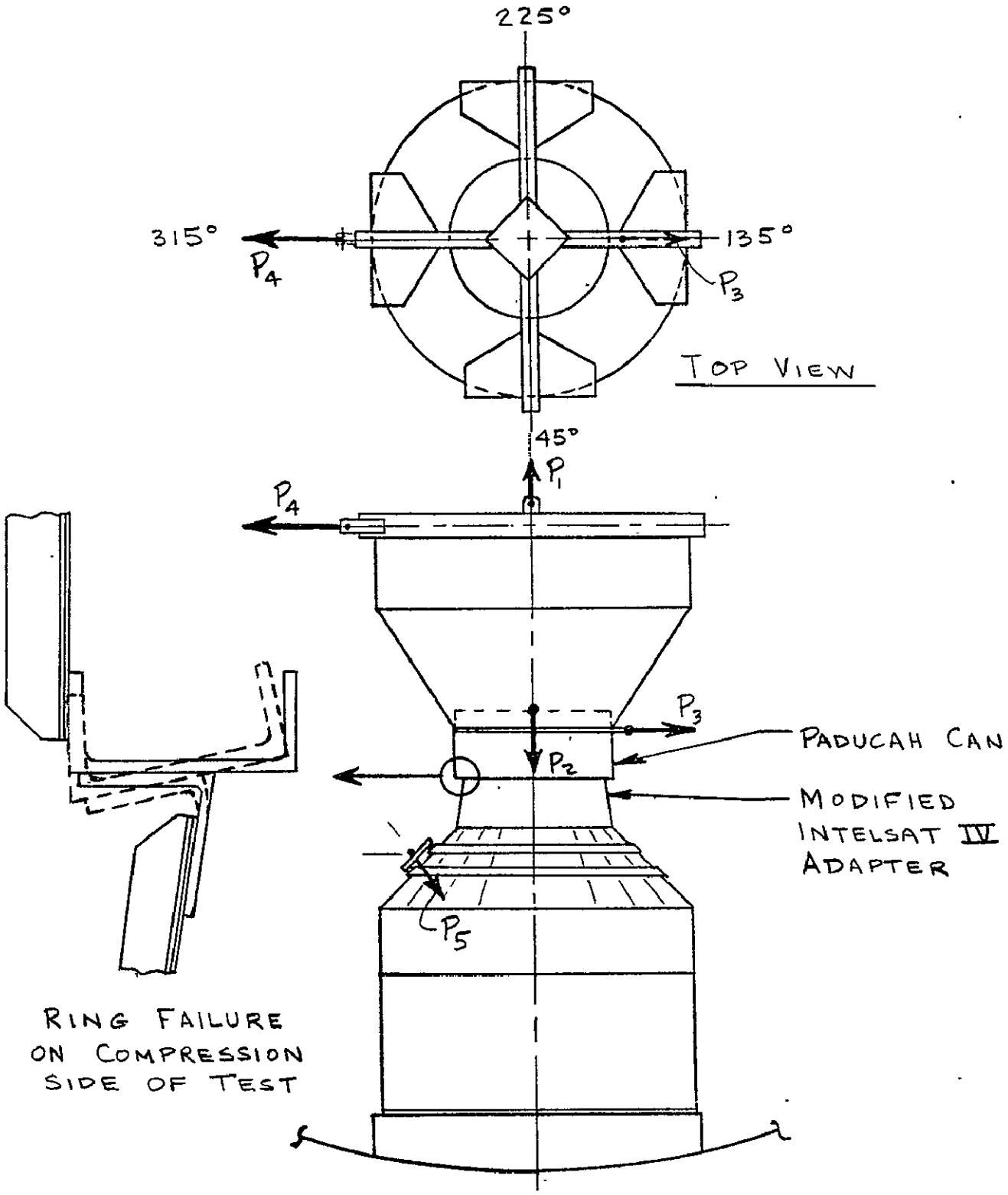

FIGURE 15 EQUIPMENT MODULE TEST WITH INTELSAT IV ADAPTER ILLUSTRATING THE TYPE OF RING FAILURE ON THE TEST HARDWARE

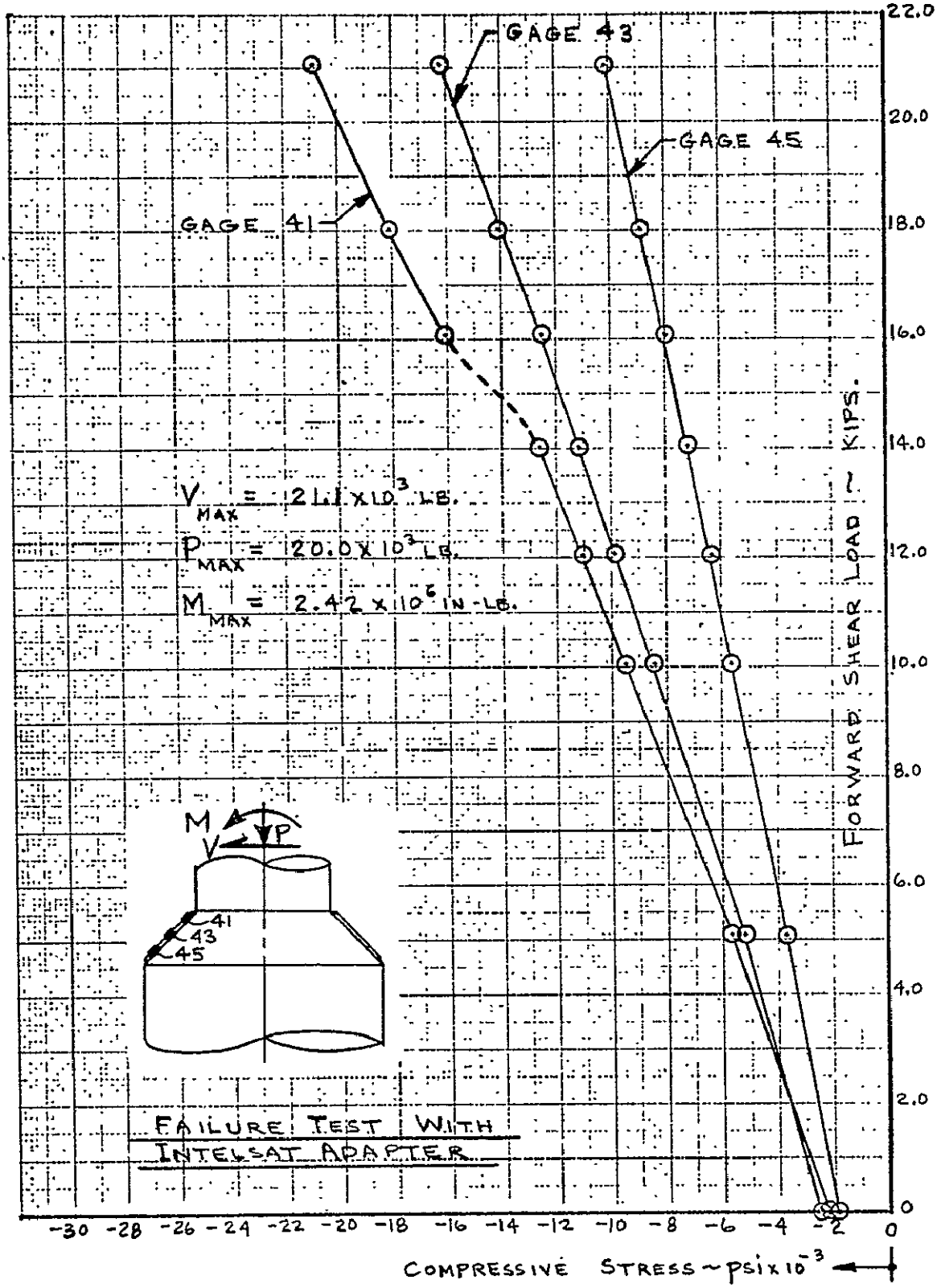

FIGURE 16 MAXIMUM COMPRESSION STIFFENER STRESS VS. FORWARD SHEAR LOAD

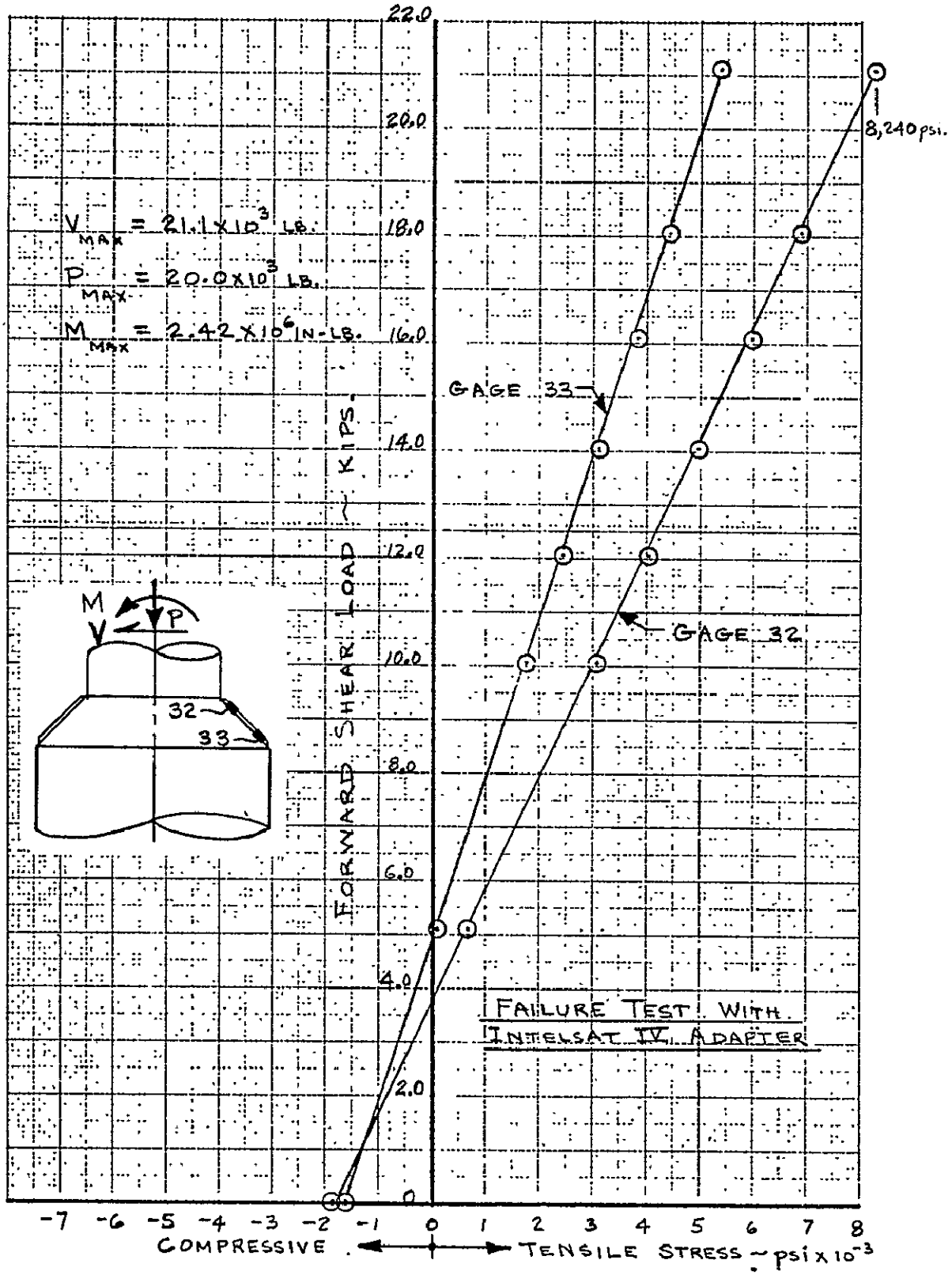

FIGURE 17 MAXIMUM TENSION STIFFENER STRESS VS. FORWARD SHEAR LOAD

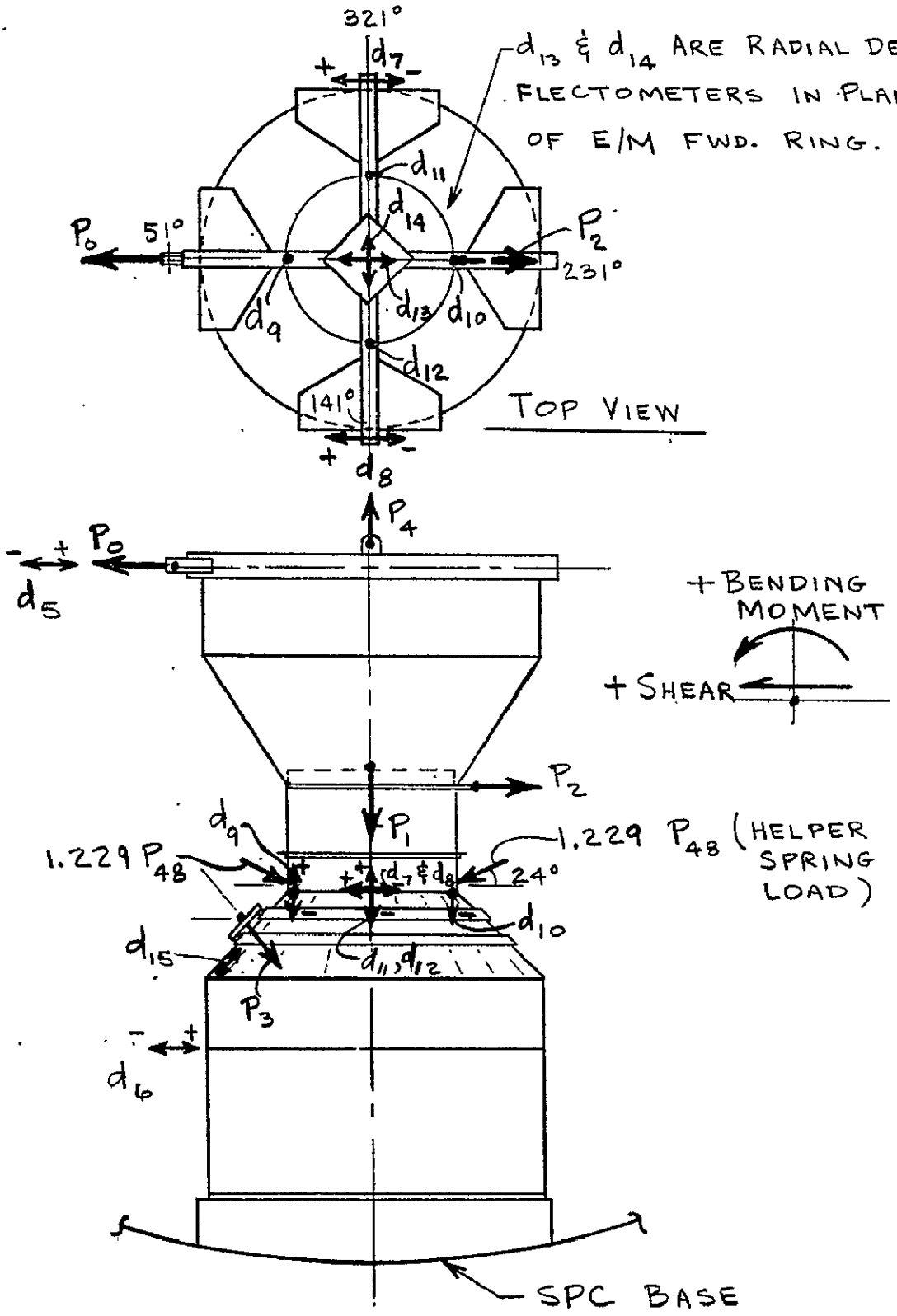

FIGURE 18 EQUIPMENT MODULE TEST WITH SIMULATED HEAD MISSION ADAPTER SHOWING DEFLECTOMETER LOCATIONS

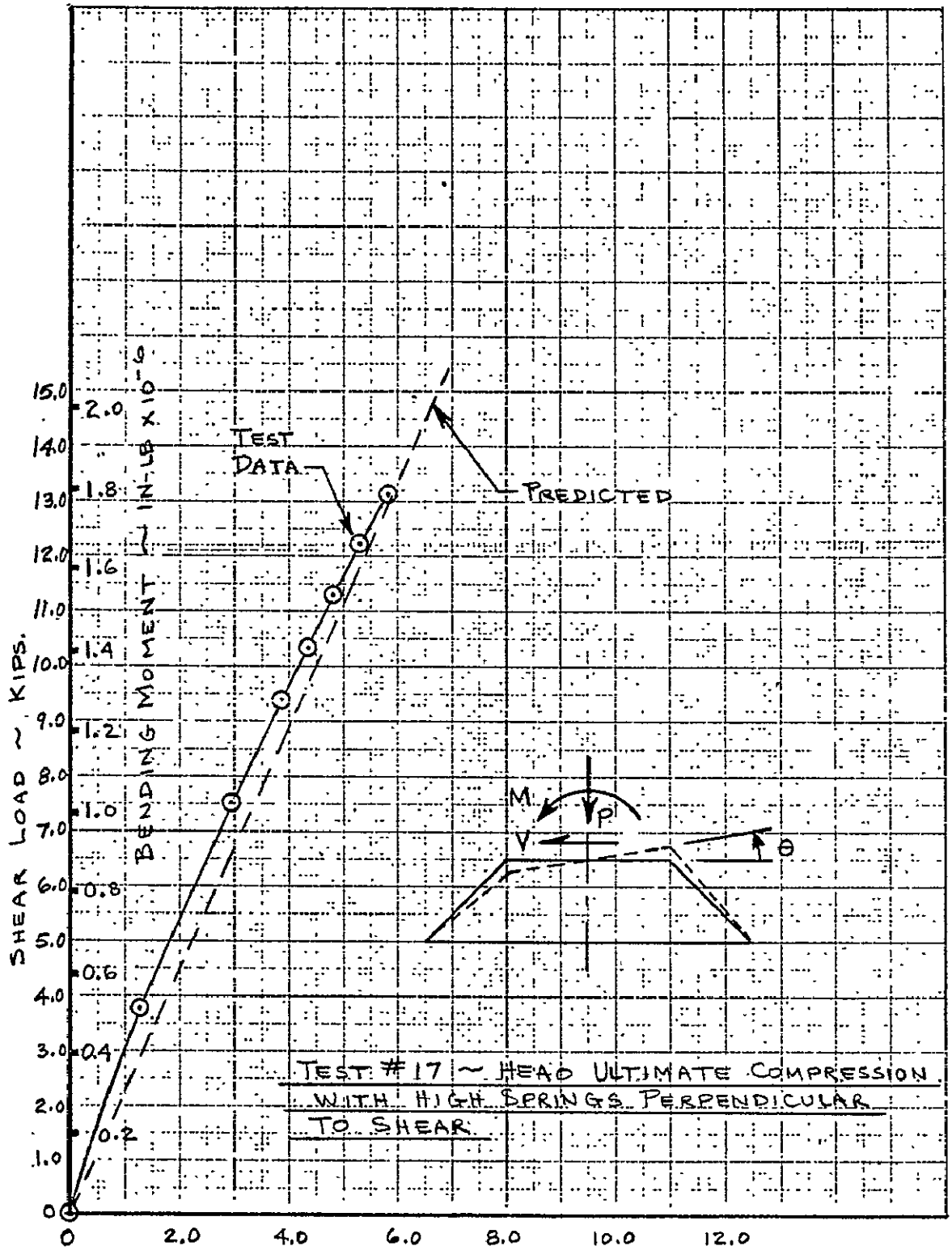

FIGURE 19 ROTATION OF E/M FORWARD RING VS. NET SHEAR AND BENDING MOMENT WITH SIMULATED HEAD ADAPTER

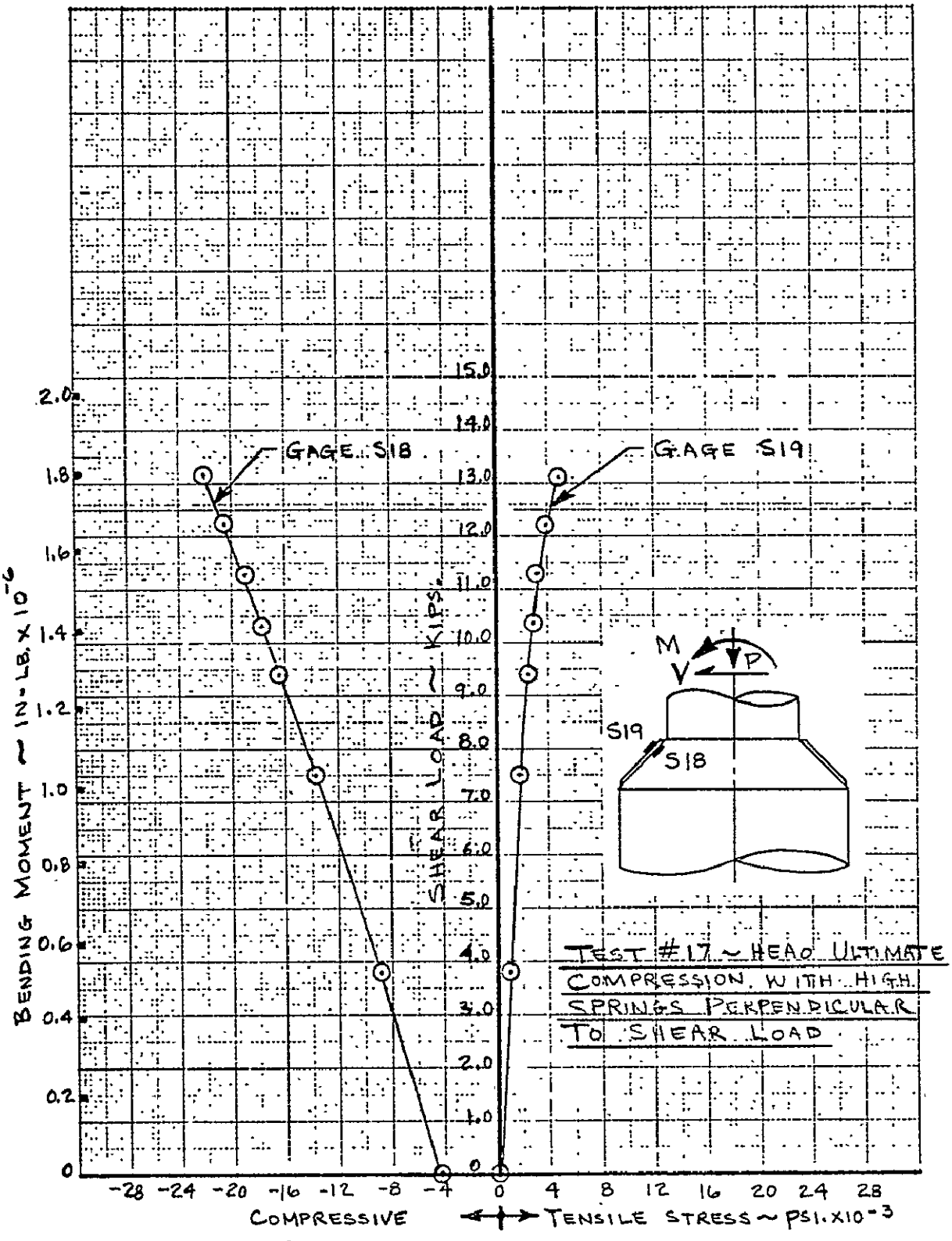

FIGURE 20 MAXIMUM COMPRESSION STIFFENER STRESS VS. SHEAR LOAD & BENDING MOMENT

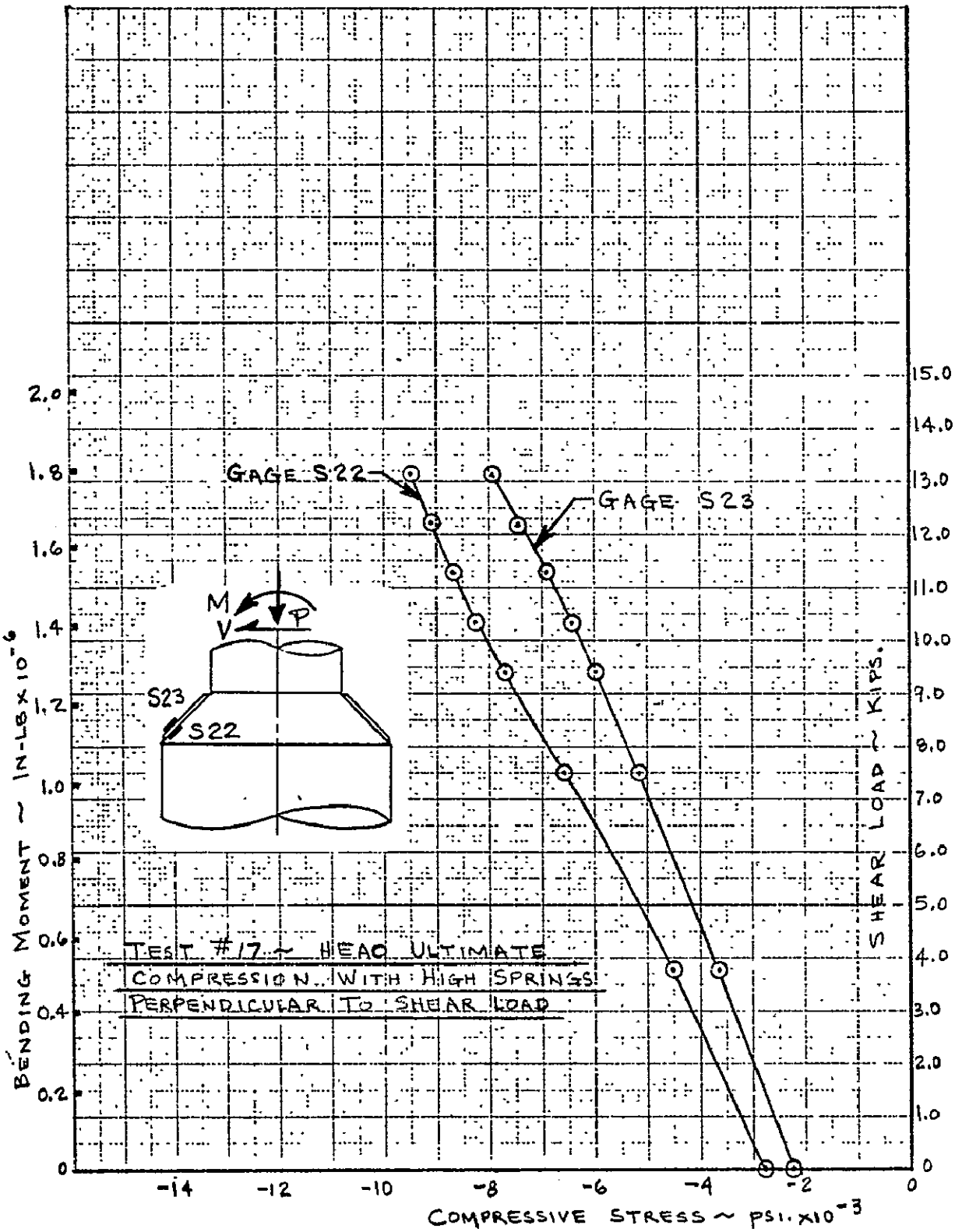

FIGURE 21 MAXIMUM COMPRESSION STIFFENER STRESS VS. SHEAR LOAD & BENDING MOMENT

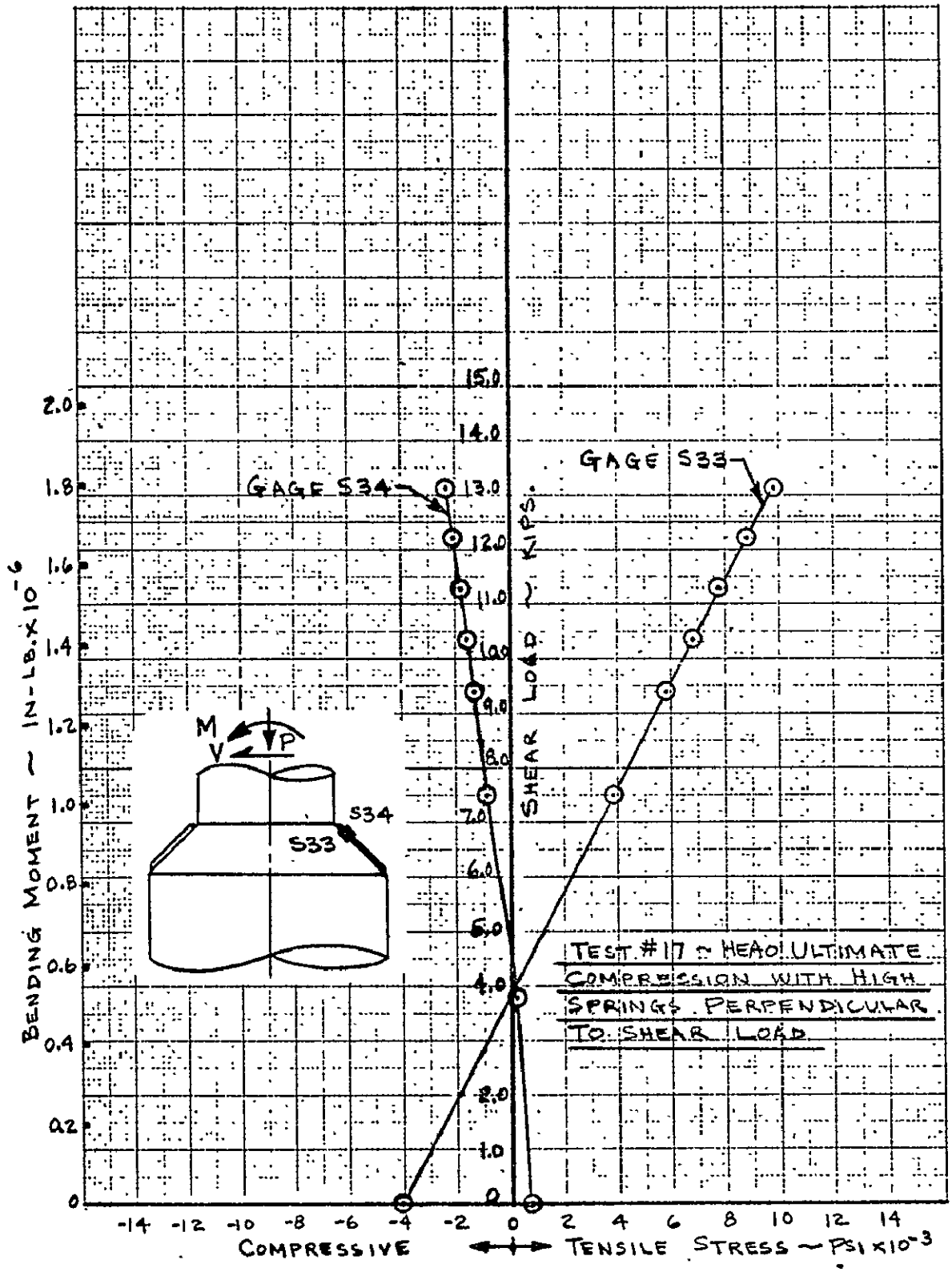

FIGURE 22 MAXIMUM TENSION STIFFENER STRESS Vs. SHEAR LOAD & BENDING MOMENT

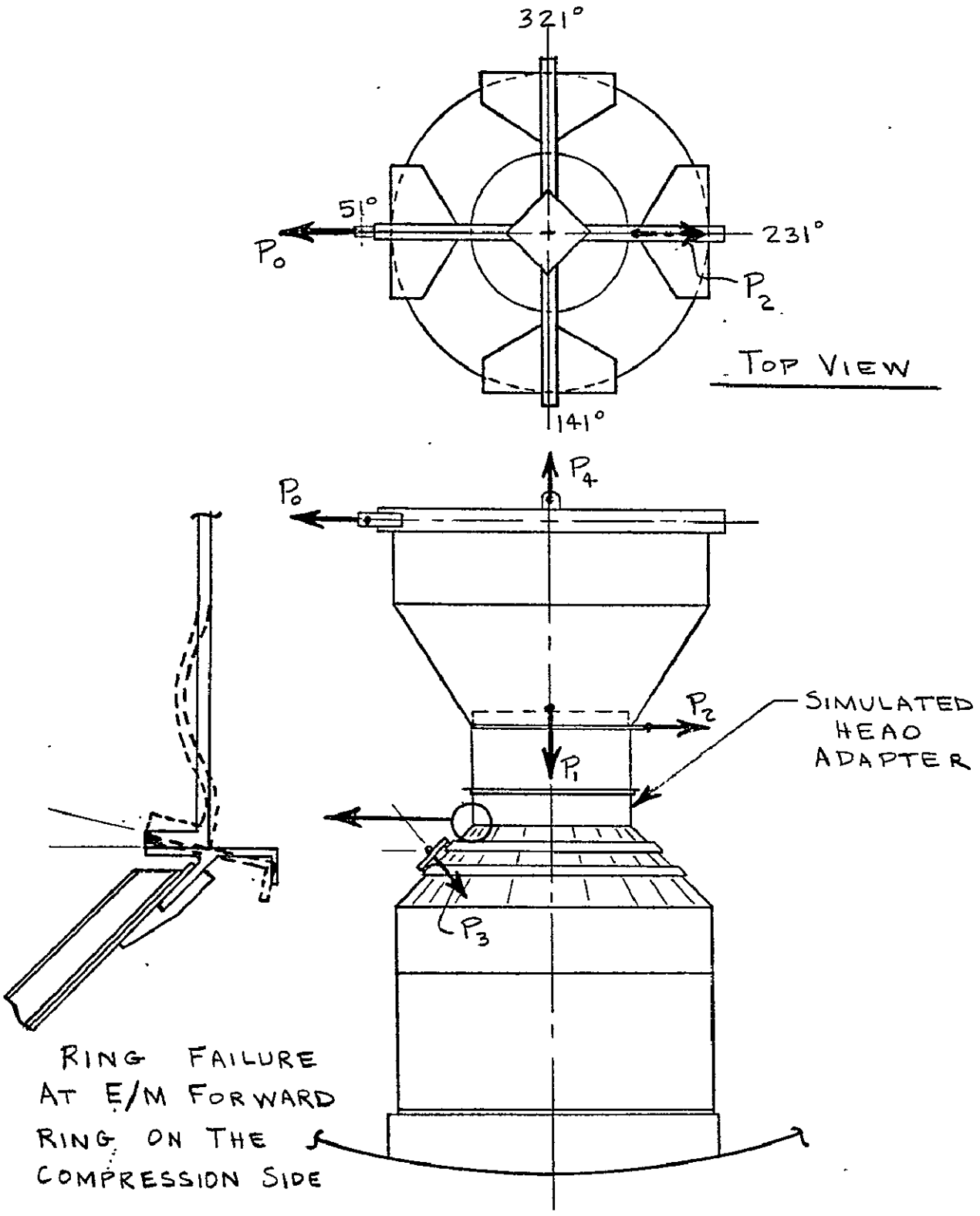

FIGURE 23 EQUIPMENT MODULE TEST WITH SIMULATED HEAD ADAPTER ILLUSTRATING THE RING FAILURE AT FORWARD E/M INTERFACE.

FIGURE 24 - EXTERNAL VIEW OF DISTORTION IN E/M FORWARD RING ON COMPRESSION SIDE

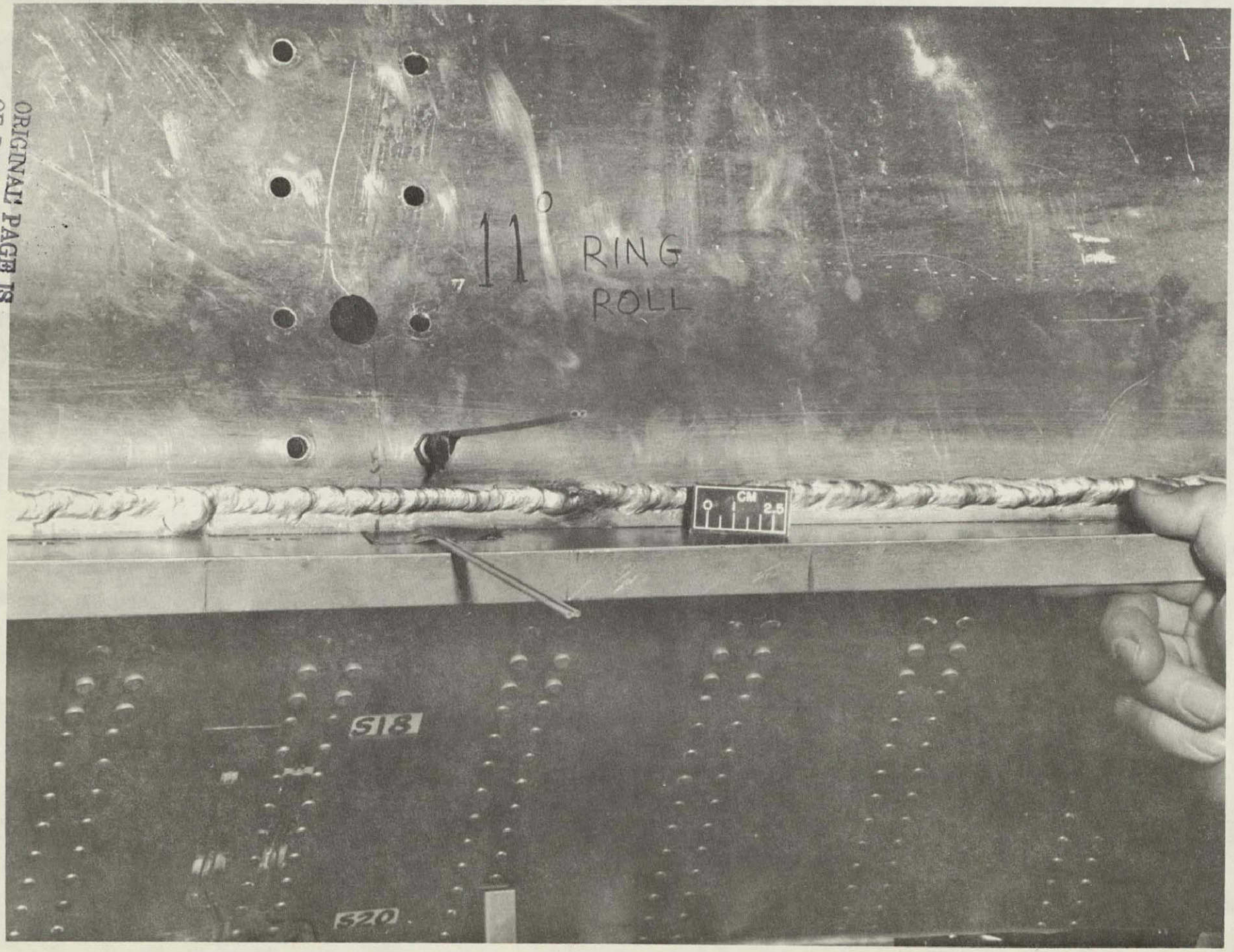

FIGURE 25 - INTERNAL VIEW OF DISTORTION IN E/M FORWARD RING ON COMPRESSION SIDE

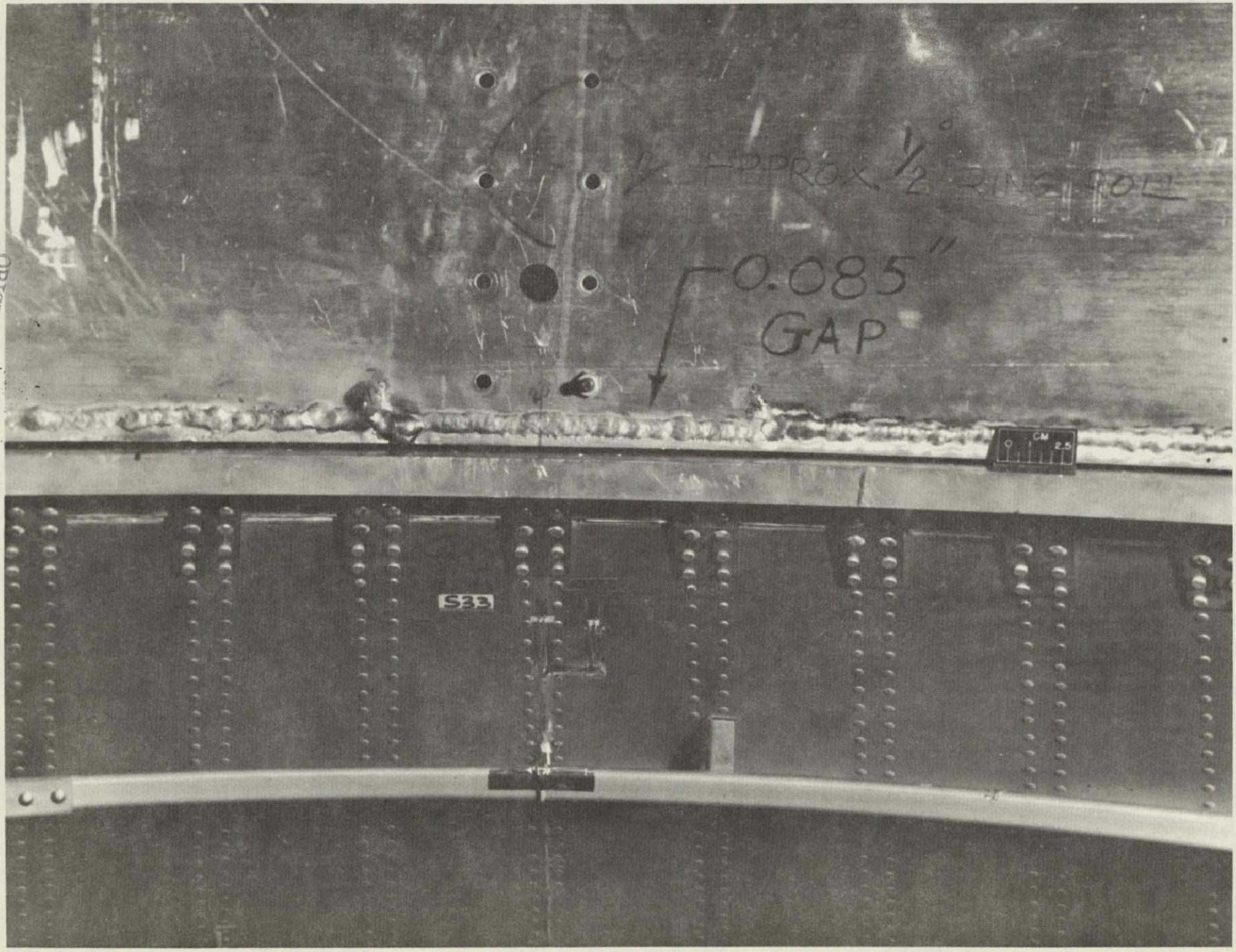

FIGURE 26 - INTERNAL VIEW OF DISTORTION IN E/M FORWARD RING ON TENSION SIDE

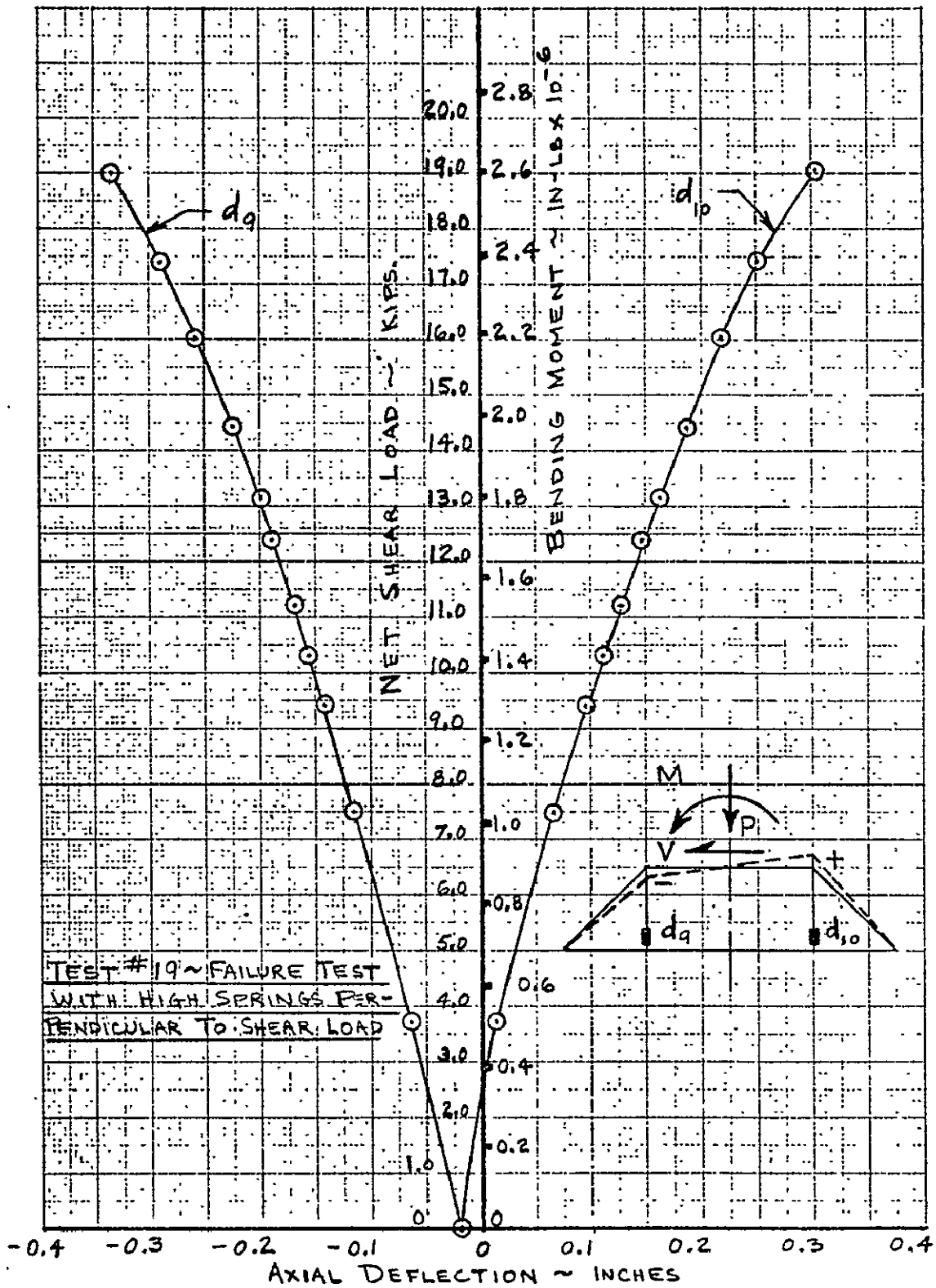

FIGURE 27 AXIAL DEFLECTION VS. NET SHEAR AND BENDING MOMENT WITH NEW SIMULATED HEAD ADAPTER

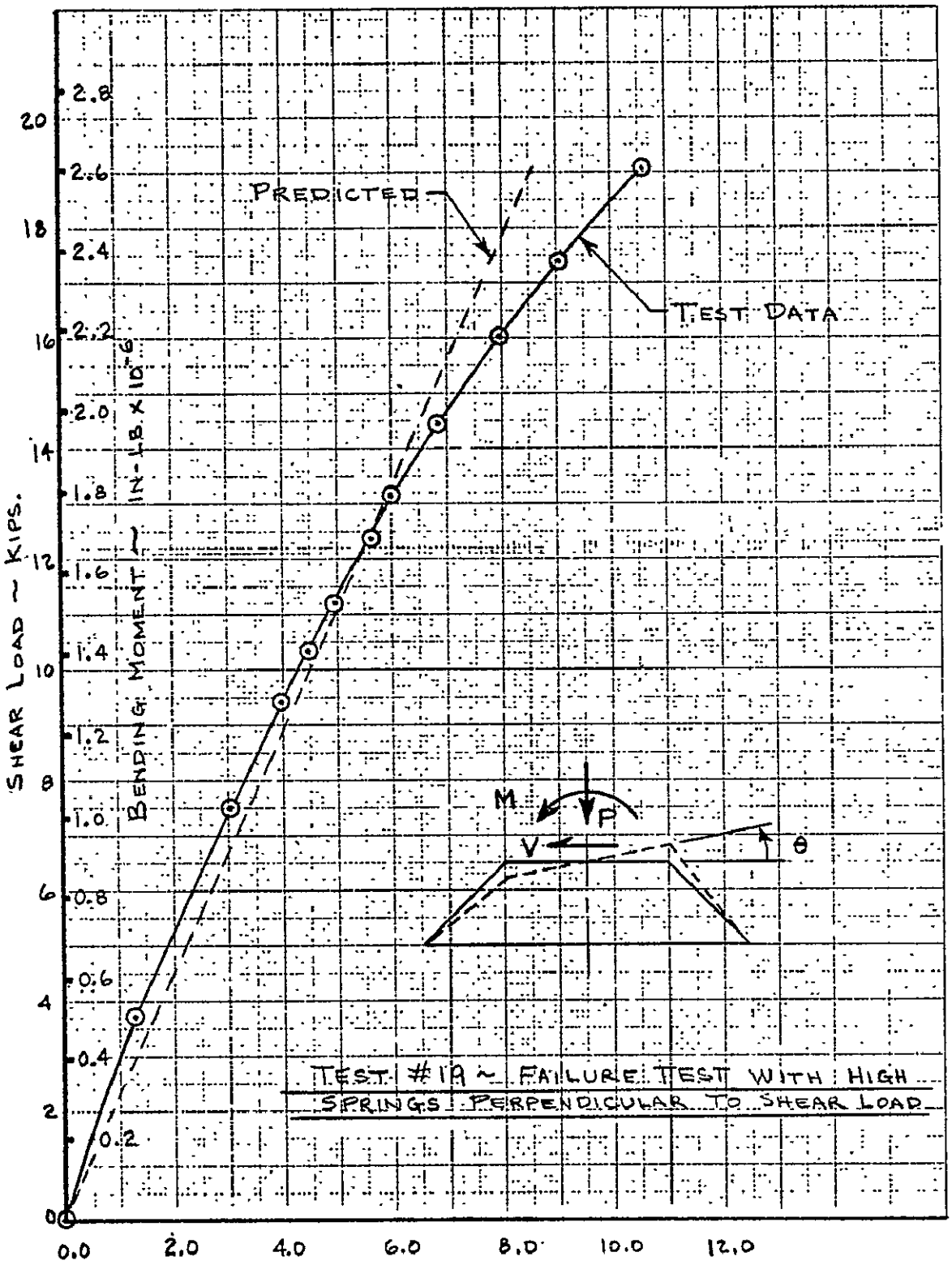

FIGURE 28 ROTATION OF E/M FORWARD RING VS. NET SHEAR AND BENDING MOMENT WITH SIMULATED HEAD ADAPTER

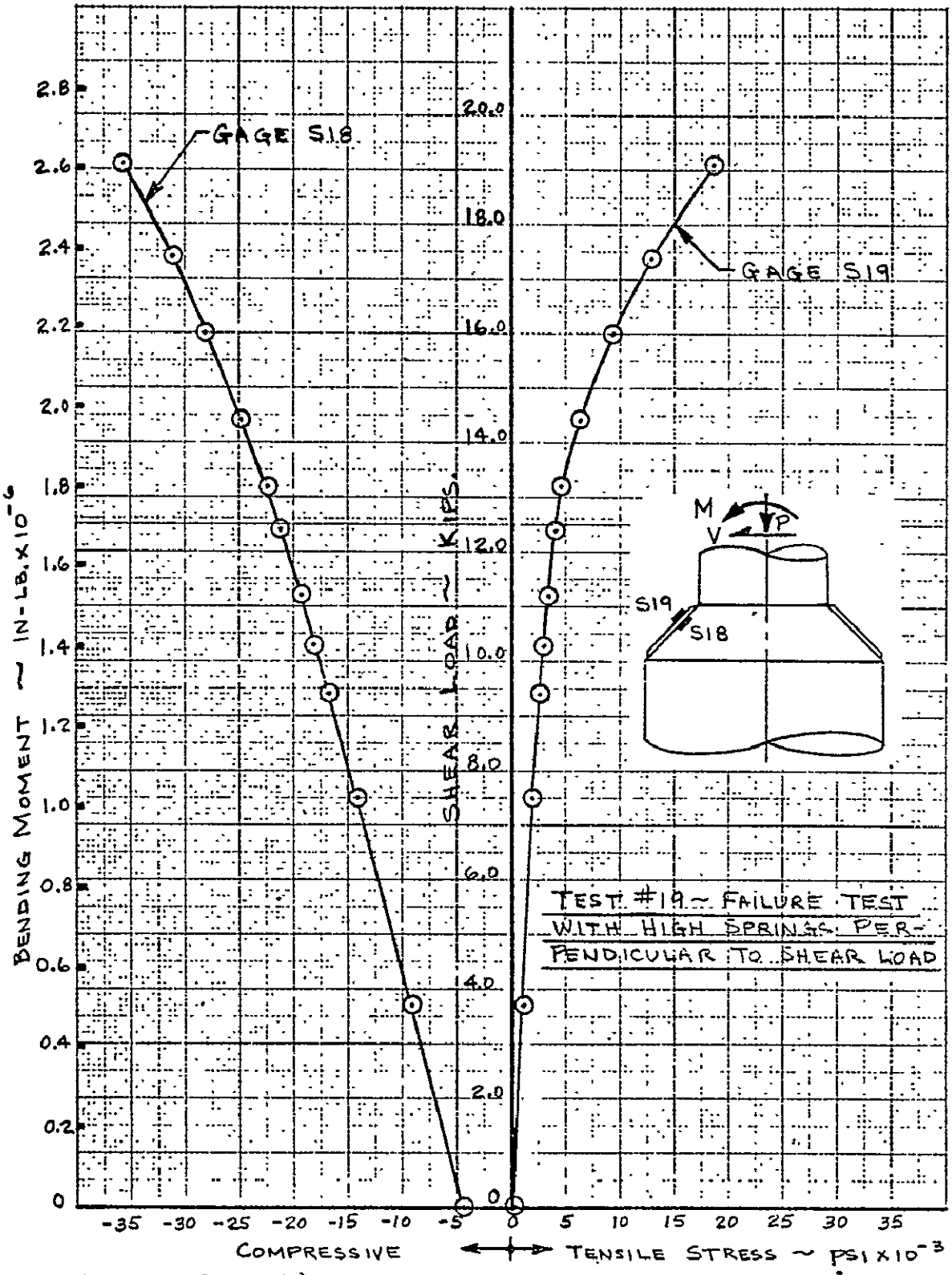

FIGURE 29 MAXIMUM COMPRESSION STIFFENER STRESS VS. SHEAR LOAD & BENDING MOMENT

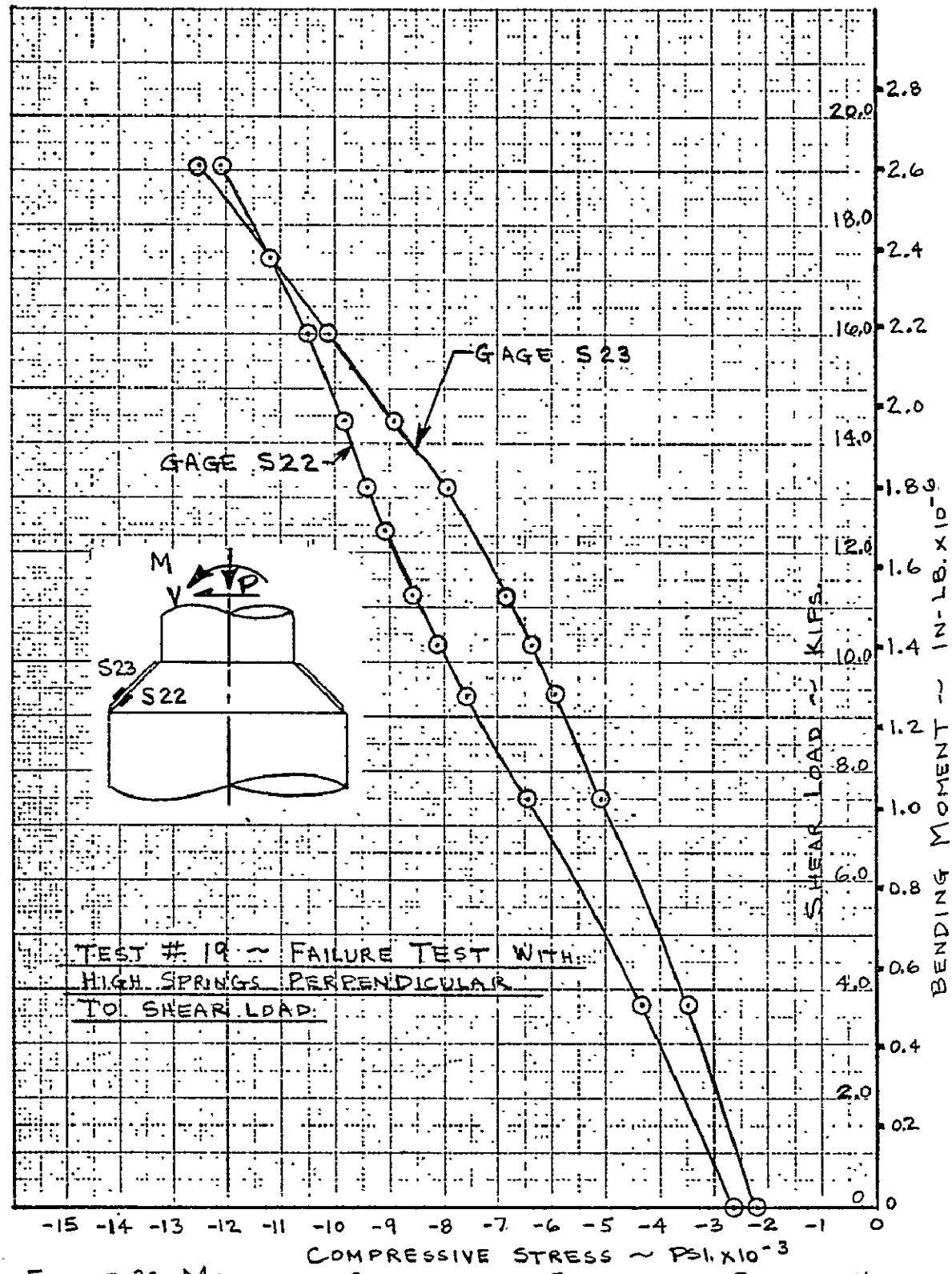

FIGURE 30 MAXIMUM COMPRESSION STIFFENER STRESS VS. SHEAR LOAD & BENDING MOMENT

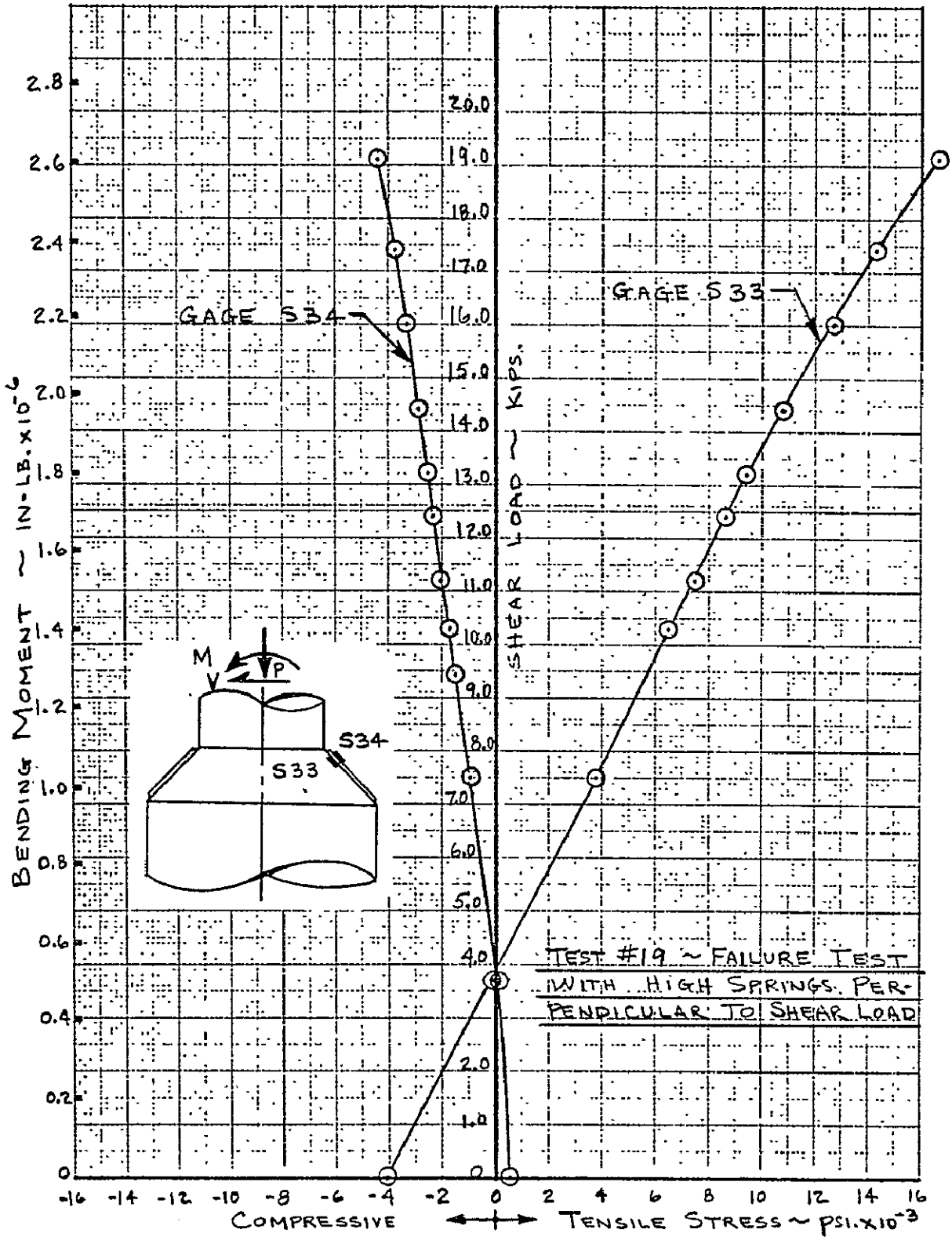

FIGURE 31 MAXIMUM TENSION STIFFENER STRESS VS. SHEAR LOAD & BENDING MOMENT

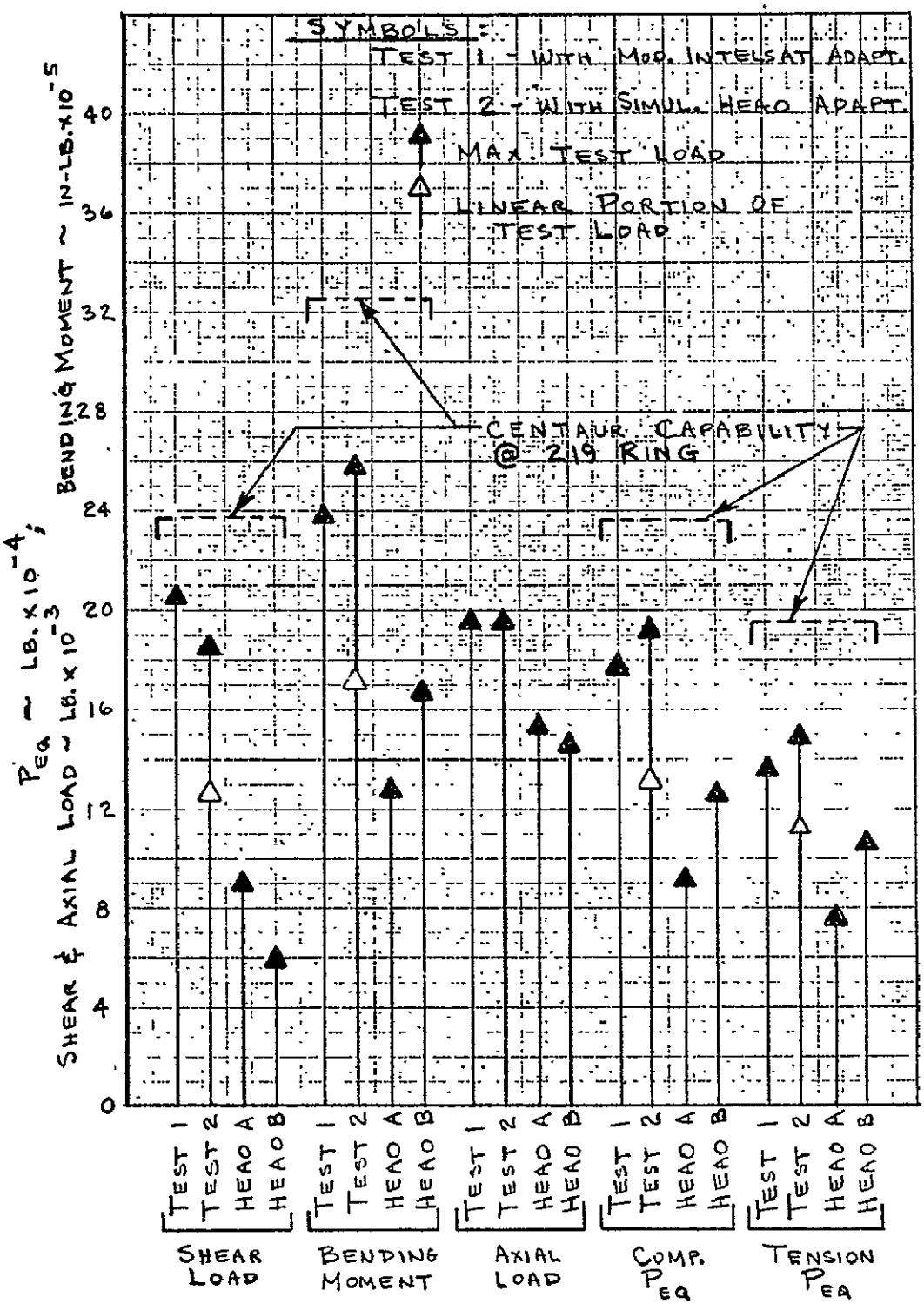

FIGURE 32 E/M TEST LOADS COMPARED TO HEAD A AND HEAD B PREDICTED FLIGHT LOADS